

Supporting Information:

Conformational plasticity of phospholipid headgroups in simulations and experiments

Amélie Bacle,[†] Pavel Buslaev,[‡] Rebeca García Fandiño,^{§,||} Fernando Favela-Rosales,[⊥] Tiago Ferreira,[#] Patrick F.J. Fuchs,^{@,△} Ivan Gushchin,[¶] Matti Javanainen,[▽] Anne M. Kiirikki,^{††} Jesper J. Madsen,^{‡‡,¶¶} Josef Melcr,^{▽,§§} Paula MilãRodríguez,^{|||} Markus S. Miettinen,^{⊥⊥} O. H. Samuli Ollila,^{*,††} Chris G. Papadopoulos,^{##} Antonio Peón,^{||} Thomas J. Piggot,^{@@} Ángel Piñeiro,^{△△} and Salla I. Virtanen^{††}

[†]*Laboratoire Coopératif "Lipotoxicity and Channelopathies - ConicMeds", Université de Poitiers, 1 rue Georges Bonnet, 86000 Poitiers, France*

[‡]*Nanoscience Center and Department of Chemistry, University of Jyväskylä, P.O. Box 35, 40014 Jyväskylä, Finland*

[¶]*Research Center for Molecular Mechanisms of Aging and Age-related Diseases, Moscow Institute of Physics and Technology, 141701 Dolgoprudny, Russia*

[§]*Center for Research in Biological Chemistry and Molecular Materials (CiQUS), Universidade de Santiago de Compostela, E-15782 Santiago de Compostela, Spain*

^{||}*CIQUP, Centro de Investigaçã em Química, Departamento de Química e Bioquímica, Faculdade de Ciências, Universidade do Porto, Porto, Portugal*

[⊥]*Departamento de Ciencias Básicas, Tecnológico Nacional de México, ITS Zacatecas Occidente, México*

[#]*Halle, Germany*

[@]*Sorbonne Université, Ecole Normale Supérieure, PSL University, CNRS, Laboratoire des Biomolécules (LBM), 75005 Paris, France*

[△]*Université de Paris, UFR Sciences du Vivant, 75013, Paris, France*

[▽]*Institute of Organic Chemistry and Biochemistry of the Czech Academy of Sciences, Flemingovo nám. 542/2, CZ-16610 Prague 6, Czech Republic*

^{††}*Institute of Biotechnology, University of Helsinki*

^{‡‡}*Department of Chemistry, The University of Chicago, Chicago, Illinois, United States of America*

^{¶¶}*Global and Planetary Health, College of Public Health, University of South Florida, Tampa, Florida, United States of America*

^{§§}*Groningen Biomolecular Sciences and Biotechnology Institute and The Zernike Institute for Advanced Materials, University of Groningen, 9747 AG Groningen, The Netherlands*

^{|||}*Sorbonne Université, Ecole Normale Supérieure, PSL University, CNRS, Laboratoire des Biomolécules (LBM), 75005 Paris, France*

^{⊥⊥}*Department of Theory and Bio-Systems, Max Planck Institute of Colloids and Interfaces, 14424 Potsdam, Germany*

^{##}*Université Paris-Saclay, CEA, CNRS, Institute for Integrative Biology of the Cell (I2BC), 91198, Gif-sur-Yvette, France*

^{@@}*Chemistry, University of Southampton, Highfield, Southampton SO17 1BJ, United Kingdom*

^{△△}*Departamento de Física Aplicada, Faculdade de Física, Universidade de Santiago de Compostela, E-15782 Santiago de Compostela, Spain*

E-mail: samuli.ollila@helsinki.fi

Contents

| | |
|---|------------|
| S1 R-PDLF and SDROSS experiments | S4 |
| S2 Lipid ligand names in PDB used in the analysis of conformations of protein-bound lipids | S6 |
| S3 Evaluation of simulations against NMR experiments | S7 |
| S3.1 Conformational ensembles of headgroup and glycerol backbone in PE and PG lipids | S7 |
| S3.2 PC headgroup in mixtures with PE or PG lipids | S10 |
| S3.3 PG headgroup in mixtures with PC lipids | S12 |
| S3.4 Calcium binding to POPC:POPG mixtures | S13 |
| S4 Dihedral angle distributions | S18 |
| S4.1 Dihedral angles of PC, PE, PG and PS headgroups | S18 |
| S4.2 Changes in headgroup conformations upon addition of charged surfactants or CaCl ₂ | S19 |
| S5 Simulated systems | S22 |
| S5.1 CHARMM36 | S25 |
| S5.2 CHARMM36-UA | S28 |
| S5.3 Slipids | S28 |
| S5.4 Berger | S31 |
| S5.5 GROMOS 43A1-S3 | S32 |
| S5.6 OPLS-UA | S32 |
| S5.7 GROMOS-CKP | S33 |
| S5.8 OPLS-MacRog | S34 |
| S5.9 Lipid17 | S36 |
| S5.10Lipid17ecc | S37 |

| | |
|--------------------------------|------------|
| S6 Author contributions | S39 |
| References | S40 |

S1 R-PDLF and SDROSS experiments

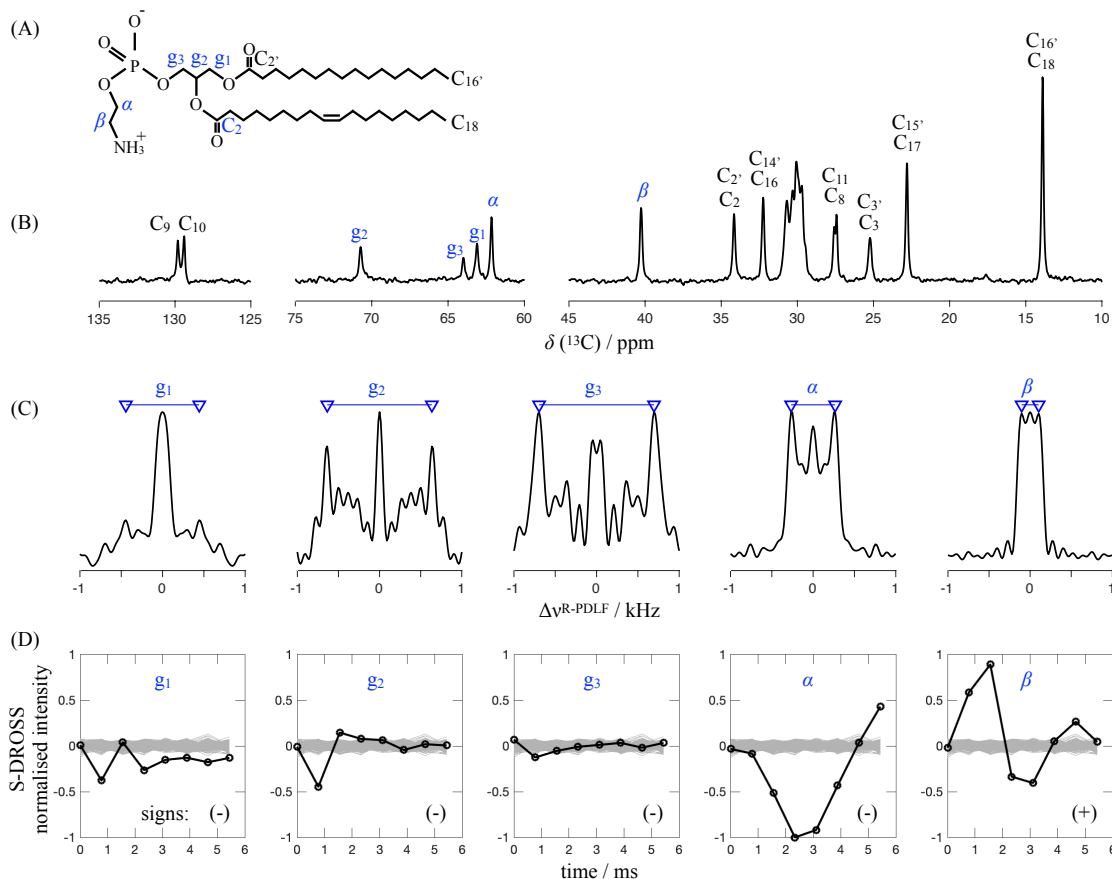


Figure S1: Solid-state NMR spectroscopy for determining the C-H bond order parameters, S_{CH} , in the POPE headgroup and glycerol backbone. (A) Chemical structure of POPE showing the labels used to identify different carbons. (B) Refocused INEPT ^{13}C spectrum of POPE MLVs. (C) Headgroup and glycerol backbone R-PDLF dipolar slices. The arrows indicate the splittings used to determine the C-H bond order parameters by using $|S_{\text{CH}}| = \Delta\nu / (0.315 \times d_{\text{CH}})$. The rigid coupling d_{CH} used was 22 kHz. (D) Experimental S-DROSS curves giving signs of the order parameters measured. Grey lines are a set of slices taken from a region of the spectrum without peaks, i.e. grey lines are noise profiles, to highlight the signal-to-noise ratio of the measured modulations.

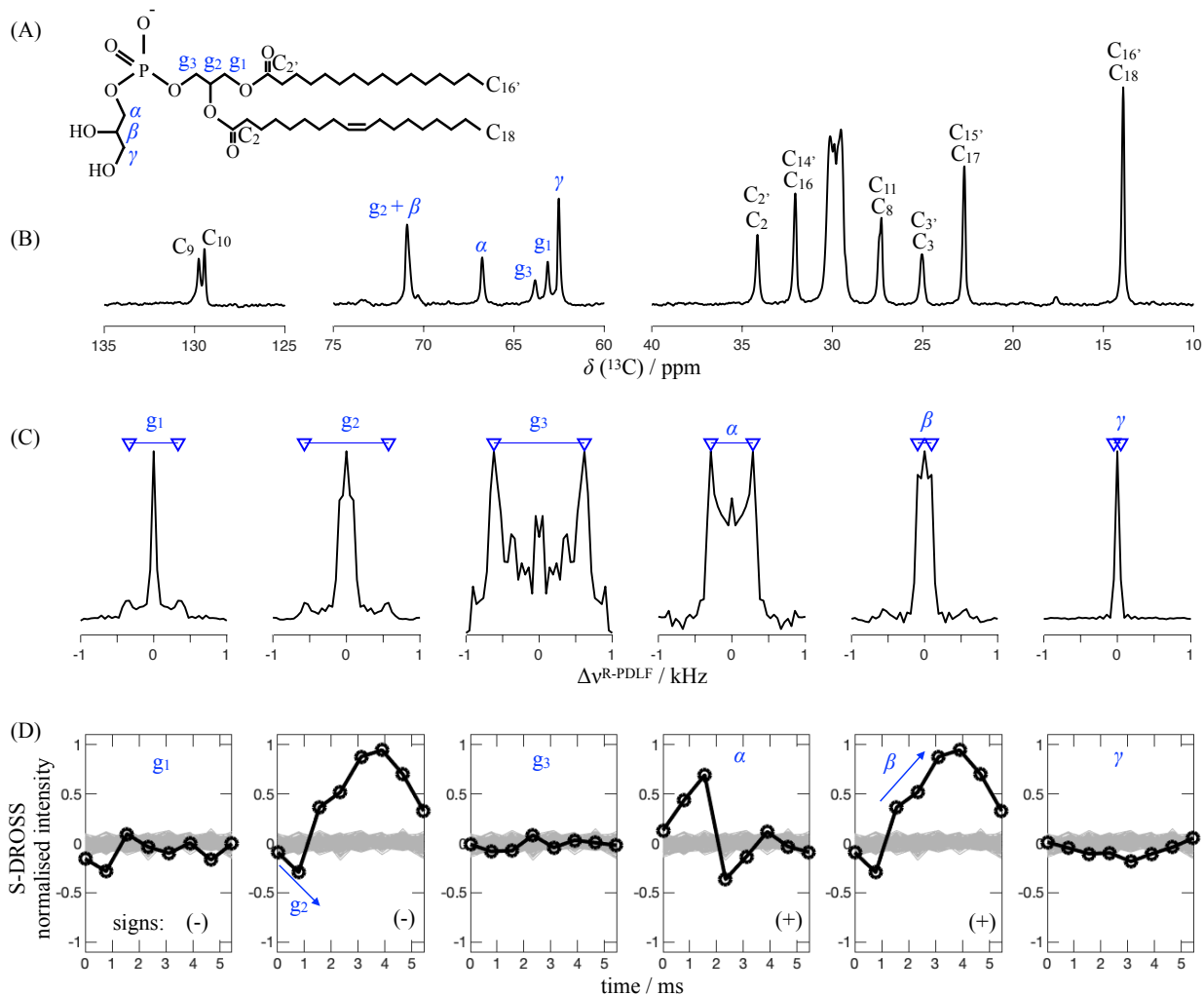


Figure S2: Solid-state NMR spectroscopy for determining the C-H bond order parameters, S_{CH} , in the POPG headgroup and glycerol backbone. (A) Chemical structure of POPG showing the labels used to identify different carbons. (B) Refocused INEPT ^{13}C spectrum of POPG MLVs. (C) Headgroup and glycerol backbone R-PDLF dipolar slices. The arrows indicate the splittings used to determine the C-H bond order parameters by using $|S_{\text{CH}}| = \Delta\nu / (0.315 \times d_{\text{CH}})$. The rigid coupling d_{CH} used was 22 kHz. (D) Experimental S-DROSS curves giving signs of the order parameters measured. Note that the S-DROSS modulation for g_3 is very close to the noise level. In this case, we have confirmed that the order parameter sign of g_3 was negative by performing a measurement with less points in the indirect dimension, more scans and using a higher MAS frequency of 8 kHz (not shown).

S2 Lipid ligand names in PDB used in the analysis of conformations of protein-bound lipids

PC: PLC, PX4, 6PL, LIO, HGX, PC7, PC8, P1O, 6O8, XP5, EGY, PLD, SBM, HXG, and PCW

PE: 8PE, PTY, 3PE, PEH, PEF, 6OE, 6O9, 9PE, PEV, 46E, SBJ, L9Q, PEK, EPH, ZPE, 9TL, 9Y0, 6OU, LOP, and PEE

PG: PGT, PGK, LHG, 44G, PGV, OZ2, D3D, PGW, DR9, P6L, PG8, H3T, and GOT

PS: PSF, PS6, Q3G, P5S, D39, PS2, 17F, and 8SP.

S3 Evaluation of simulations against NMR experiments

S3.1 Conformational ensembles of headgroup and glycerol backbone in PE and PG lipids

The quality of PE and PG headgroup conformational ensembles in different simulations are evaluated against NMR experiments in figures S3 and S4 using C-H bond order parameters as in our previous studies for PC and PS lipids.^{1,2} Conclusions are the same for all lipids: None of the force fields correctly captures the lipid headgroup conformational ensembles, but CHARMM36 gives results closest to experiments. Most importantly for this work, the CHARMM36 captures the distinct headgroup order parameters for PG and PS lipids observed in NMR experiments (Figs. 1 and 2 in the main text). It should be noted that the PG headgroup is biologically abundant R enantiomer in all simulations, while our ¹³C NMR experiments has a racemic mixture. Nevertheless, previous ²H NMR experiments comparing results between different enantiomers concluded that the structural differences between these are minor.³

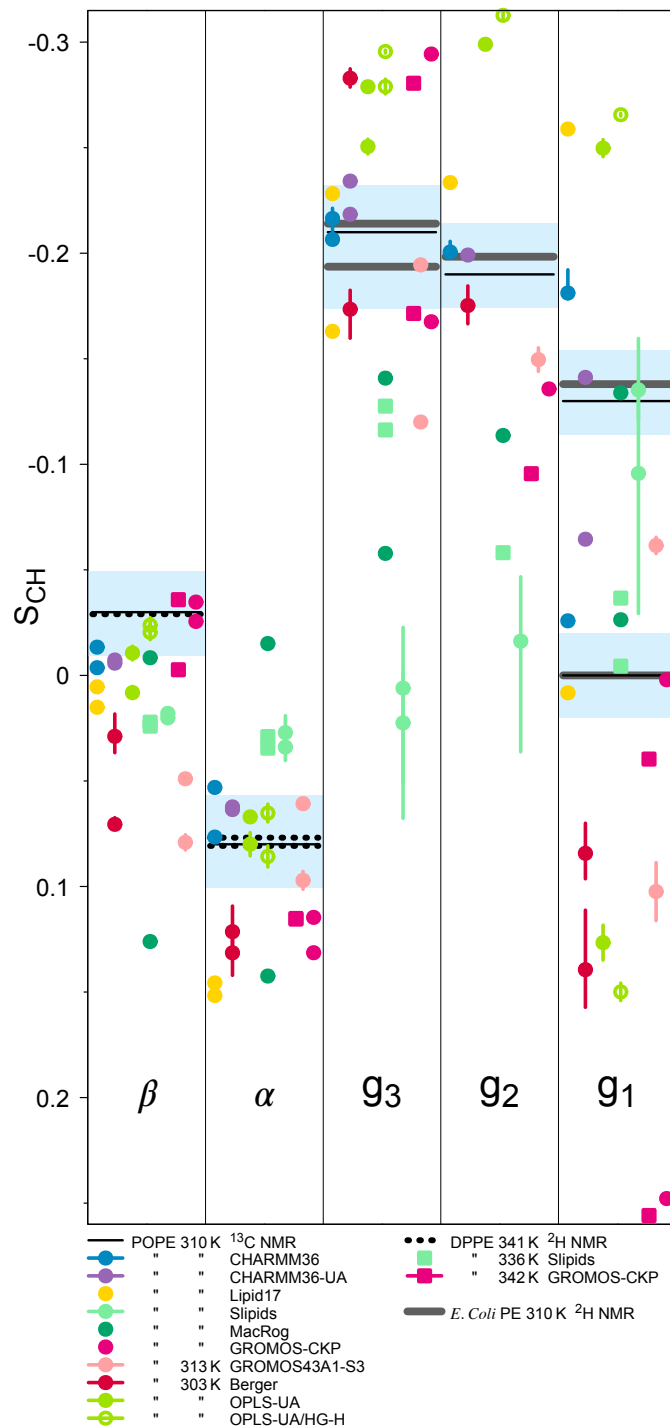


Figure S3: C–H bond order parameters, S_{CH} , of the PE headgroup (β and α) and glycerol backbone (g_3 , g_2 , g_1) carbons from NMR experiments (horizontal lines; POPE and signs this work, DPPE from Ref. 4, *Escherichia coli* PE from Ref. 5) and MD simulations with different force fields (symbols). The light blue areas span 0.04 units around the average of the extremal experimental values, in accordance with the expected quantitative accuracy of experiments.⁶ The vertical bars shown for most simulation values are not error bars, but demonstrate that for these systems we had at least two data sets; the ends of the bars mark the extreme values from the sets, the symbol marks the measurement-time-weighted average.

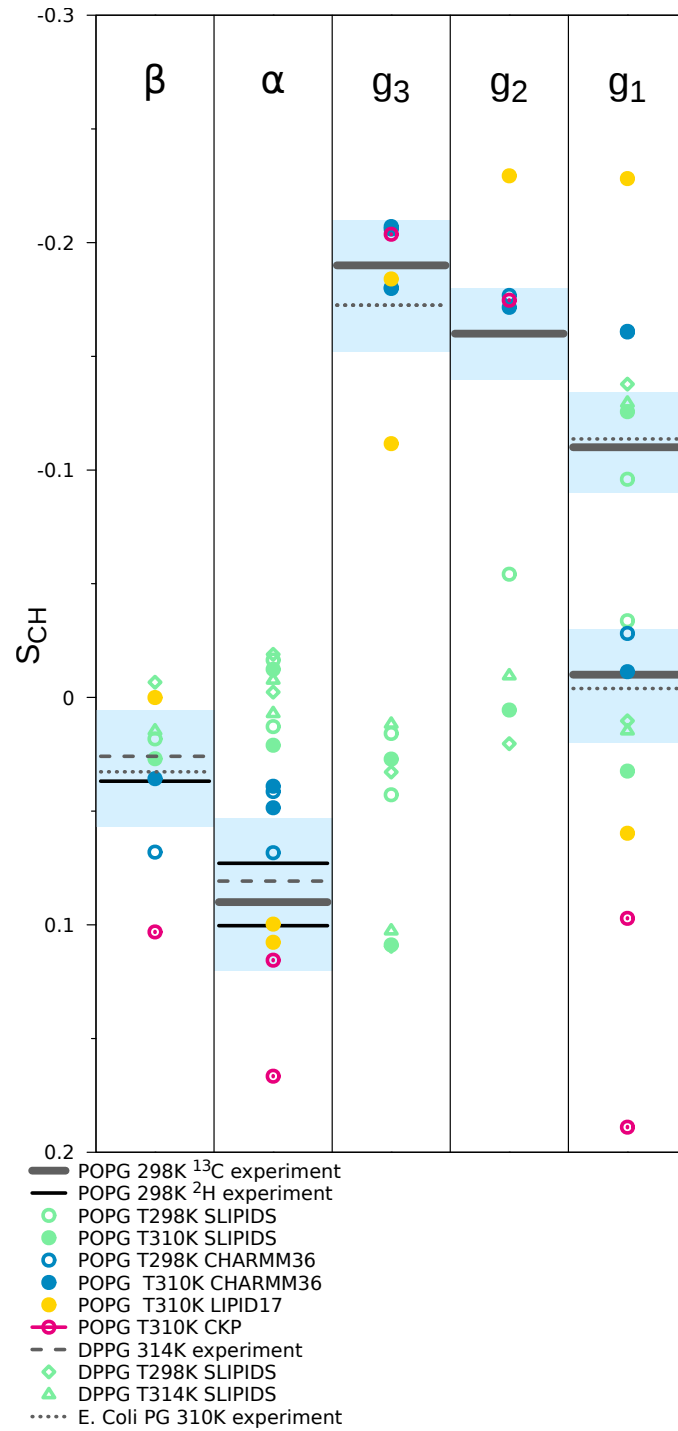


Figure S4: The headgroup and glycerol backbone order parameters of PG lipids from experiments (POPG and signs from this work and from Ref. 7, DPPG with 100mM NaCl from Ref. 3, and E. Coli PG results from Ref. 5) and simulations with different force fields.

S3.2 PC headgroup in mixtures with PE or PG lipids

Headgroup order parameters of PC lipids are unchanged upon addition of zwitterionic lipids or cholesterol in experiments, but increase upon addition of negatively charged PG or PS lipids because headgroup dipole tilts more parallel to the membrane plane after incorporation of negative charges into the membrane.^{2,8,10} The response of PC headgroup order parameters to the addition of PE or PG lipids from different simulations is compared with experiments in figure S5. None of the simulations reproduce neither the experimentally observed increase in PC headgroup order parameters with increasing amount of PG nor the related tilting of the headgroup more parallel with the membrane. Similar observations in our previous work for PS lipids were explained by the overestimated counterion binding affinity that neutralizes the effect of added negative charge.² All simulations except Berger-OPLS predict tilting of P-N headgroup outwards from the membrane and decrease of PC headgroup order parameters upon addition of PE lipids. These results are not in line with experiments where the PC headgroup order parameters are not affected by zwitterionic lipids.⁸ The good performance of Berger-OPLS simulations is surprising here because headgroup conformational ensemble is not very close to experiments in this model and the response of headgroup order parameters to cholesterol was significantly overestimated by the Berger/Höltje force field in our previous work.¹

In conclusion, more accurate force fields are needed to correctly simulate the interactions between different headgroups.



Figure S5: Modulation of POPC headgroup order parameters with increasing amount of POPE (left) and POPG (right) in bilayer from experiments at 298 K^{8,9} and simulations with different force fields (temperatures listed in tables S3 and ?? are between 298-310 K). Signs are determined as discussed in Refs. 1,6.

S3.3 PG headgroup in mixtures with PC lipids

Changes in other than PC lipid headgroup with changing membrane composition are less extensively characterized in the literature. The β -carbon order parameter in PG headgroup increases mildly⁹ or is unchanged⁷ upon increasing amount of PC lipids (Fig. S6), but experimental data from α -carbon is not available. Also the tested force fields predict very small changes for the β -carbon order parameter, while the P-N vector tilt and its response to the increased amount of PC varies significantly between force fields in figure S6. Therefore, more experimental data and more accurate force fields are still required to resolve the PG conformational ensembles in mixtures with other lipids.



Figure S6: Modulation of PG lipid headgroup order parameters with the increasing amount of PC in lipid bilayer from experiments at 298 K^{7,9} and simulations with different force fields at 310 K.

S3.4 Calcium binding to POPC:POPG mixtures

The changes of headgroup order parameters in POPC:POPG mixtures upon addition of CaCl_2 between different simulations and experiments^{7,9} are compared in figures S7 (molar ratio 1:1) and S9 (molar ratio 4:1). The results are in line with our previous studies: most force fields overestimate the calcium binding,^{2,11} but CHARMM36 with the NBfix correction underestimates the binding affinity,² and the implicit inclusion of electronic polarizability using the electronic continuum correction (ECC) improves the results.^{12,13}

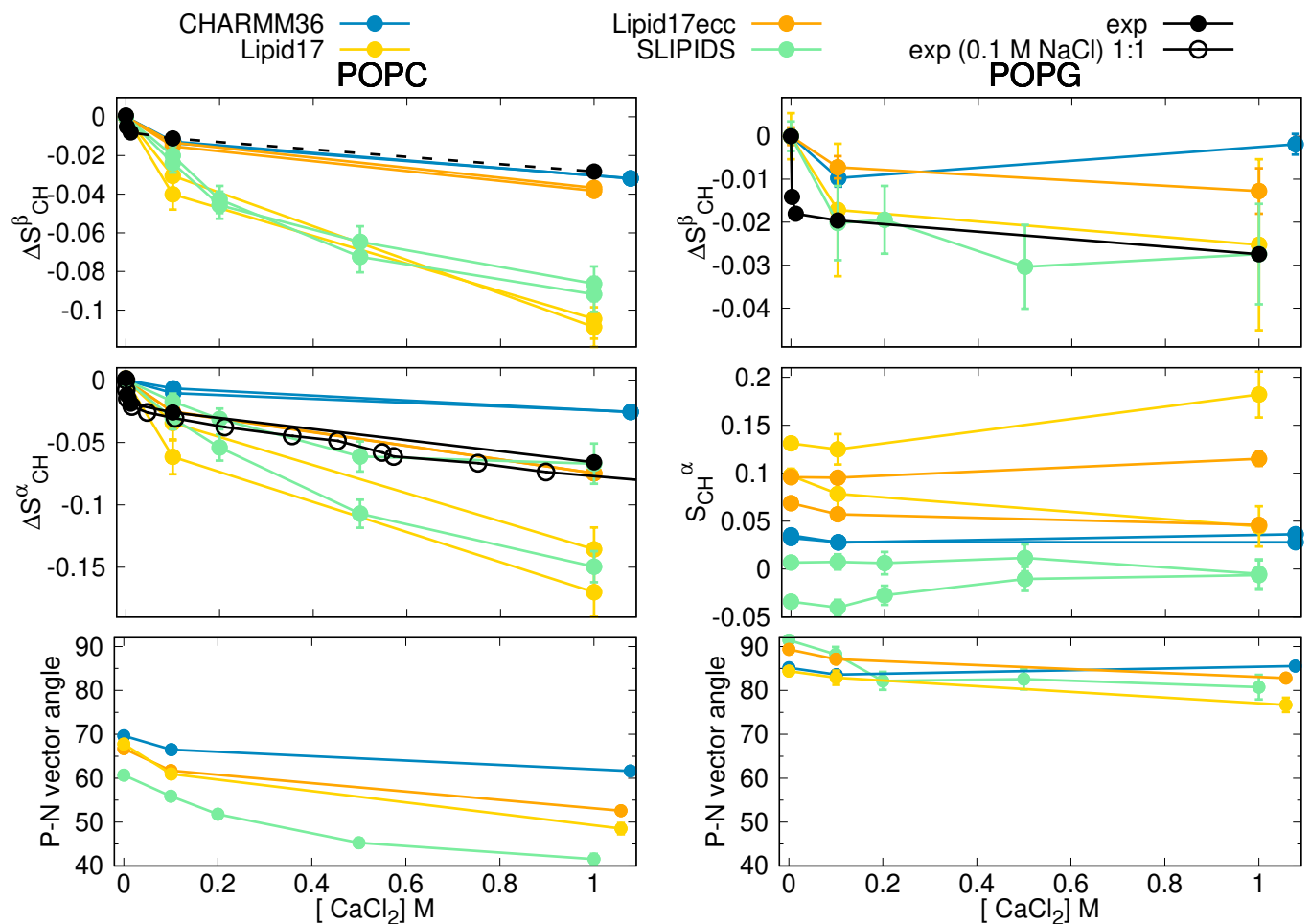


Figure S7: Modulation of headgroup order parameters of POPC (*left*) and POPG (*right*) in POPC:POPG (1:1) mixture upon addition of CaCl_2 in 298 K temperature from experiments^{7,9} and simulations. The β -carbon order parameter of POPC (dashed line on top left) is not directly measured but calculated from empirical relation $\Delta S_\beta = 0.43\Delta S_\alpha$.¹⁴ The changes with respect to the systems without CaCl_2 are shown for other data than for the α -carbon of POPG for which experimental order parameter is not available. Calcium density distributions are shown in figure S8.

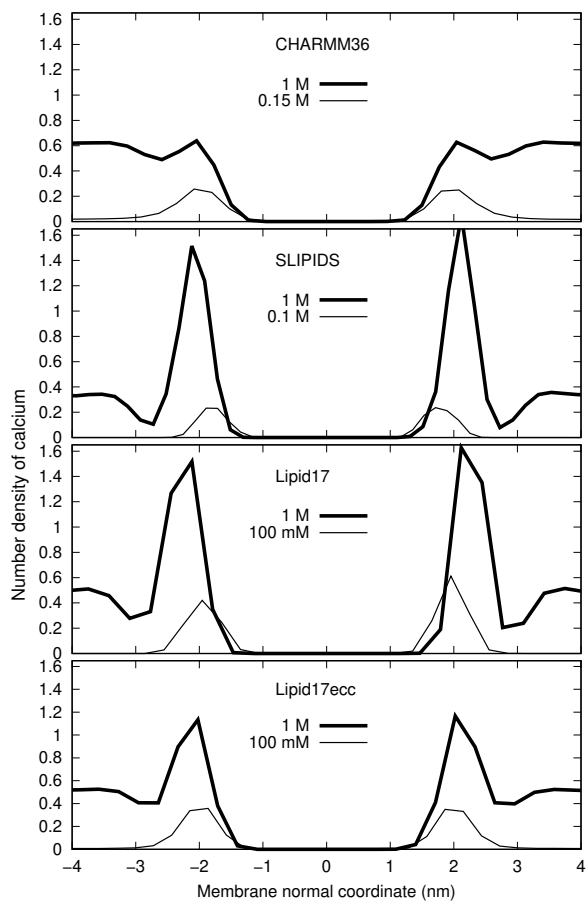
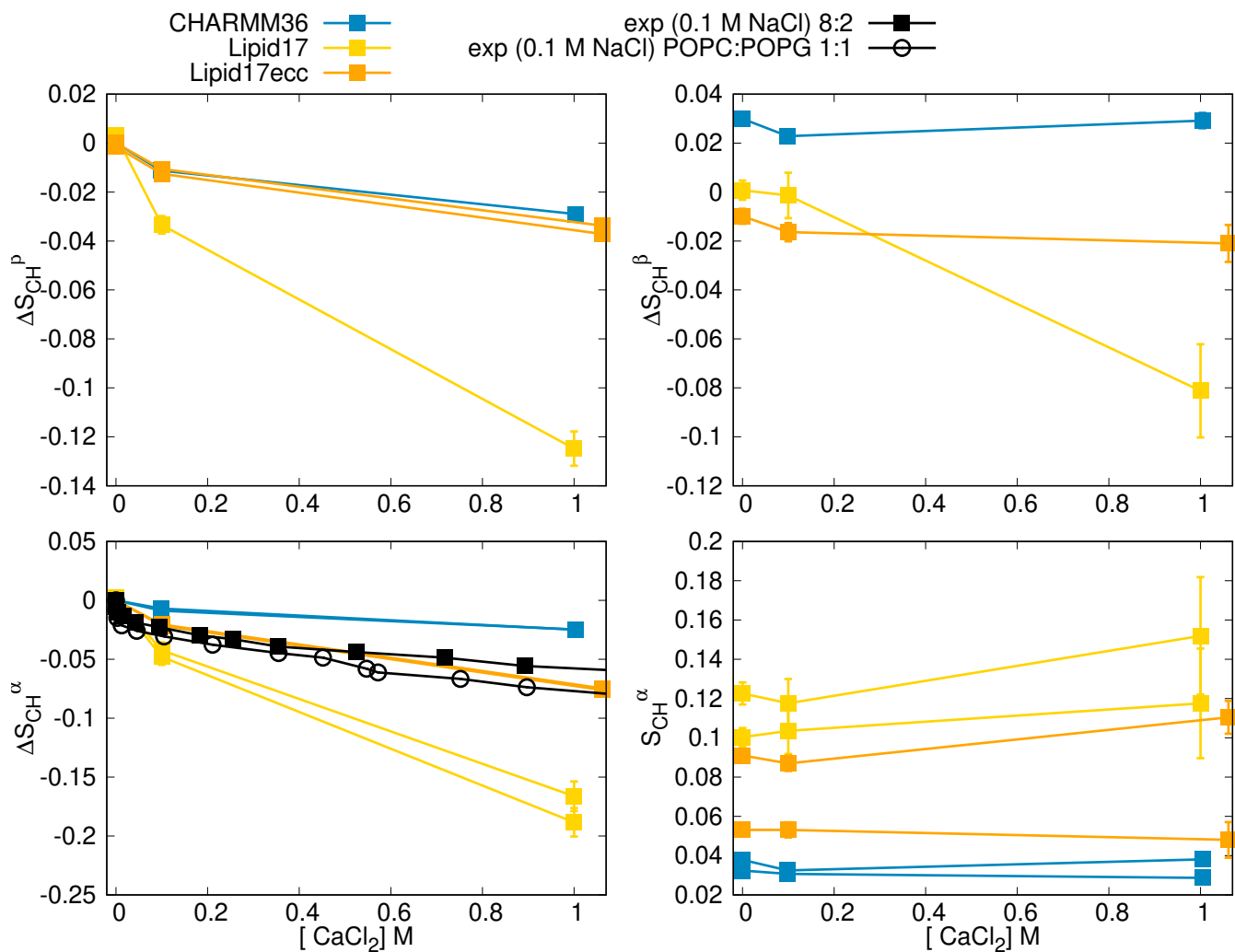


Figure S8: Calcium ion density profiles along membrane normal from simulations of POPC:POPG (1:1) mixtures with different force fields. The changes in the order parameters upon addition of CaCl_2 are compared with experiments in figure S7.



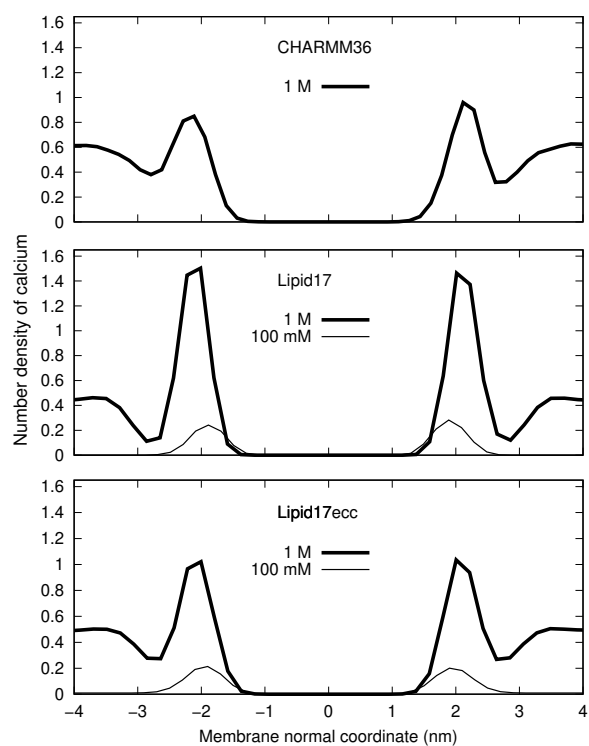


Figure S10: Calcium ion density profiles along membrane normal from simulations of POPC:POPG (4:1) mixtures with different force fields.

S4 Dihedral angle distributions

S4.1 Dihedral angles of PC, PE, PG and PS headgroups

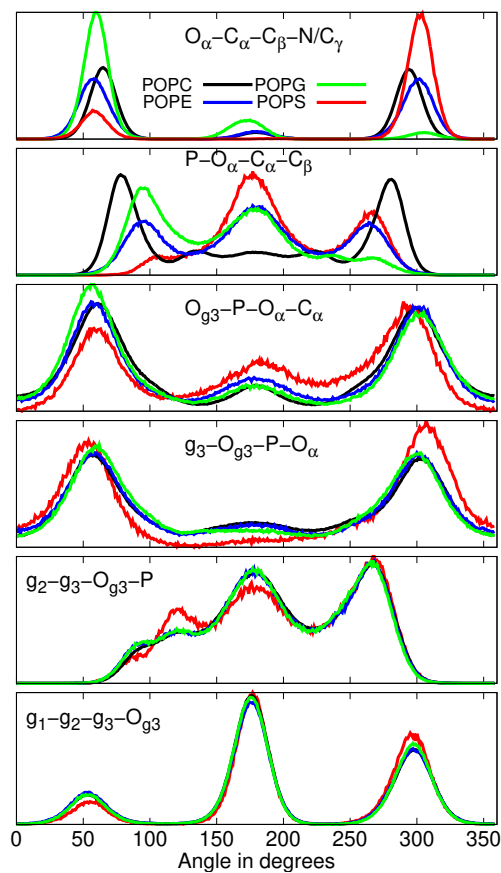


Figure S11: Heavy atom dihedral angle distributions from CHARMM36 simulations that correctly capture the order parameter differences between lipid headgroups.

S4.2 Changes in headgroup conformations upon addition of charged surfactants or CaCl_2

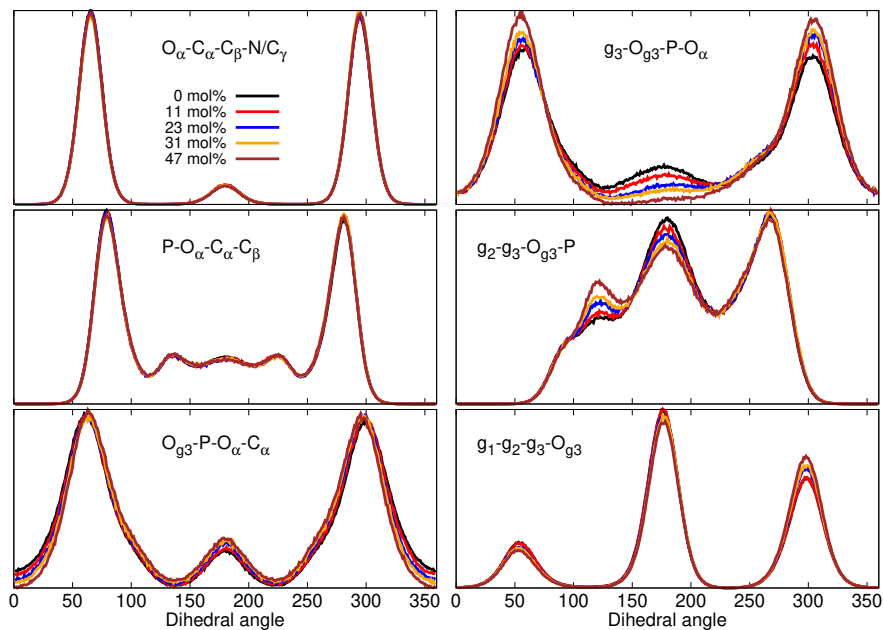


Figure S12: Changes in PC headgroup conformational ensembles upon increasing the amount of positive charge in bilayer, characterized by the heavy atom dihedral distributions, from CHARMM36 simulations.



Figure S13: Changes in POPC lipid17ecc dihedrals with increasing amount of CaCl_2 .



Figure S14: Changes in POPC CHARMM36 dihedrals with increasing amount of CaCl_2 .

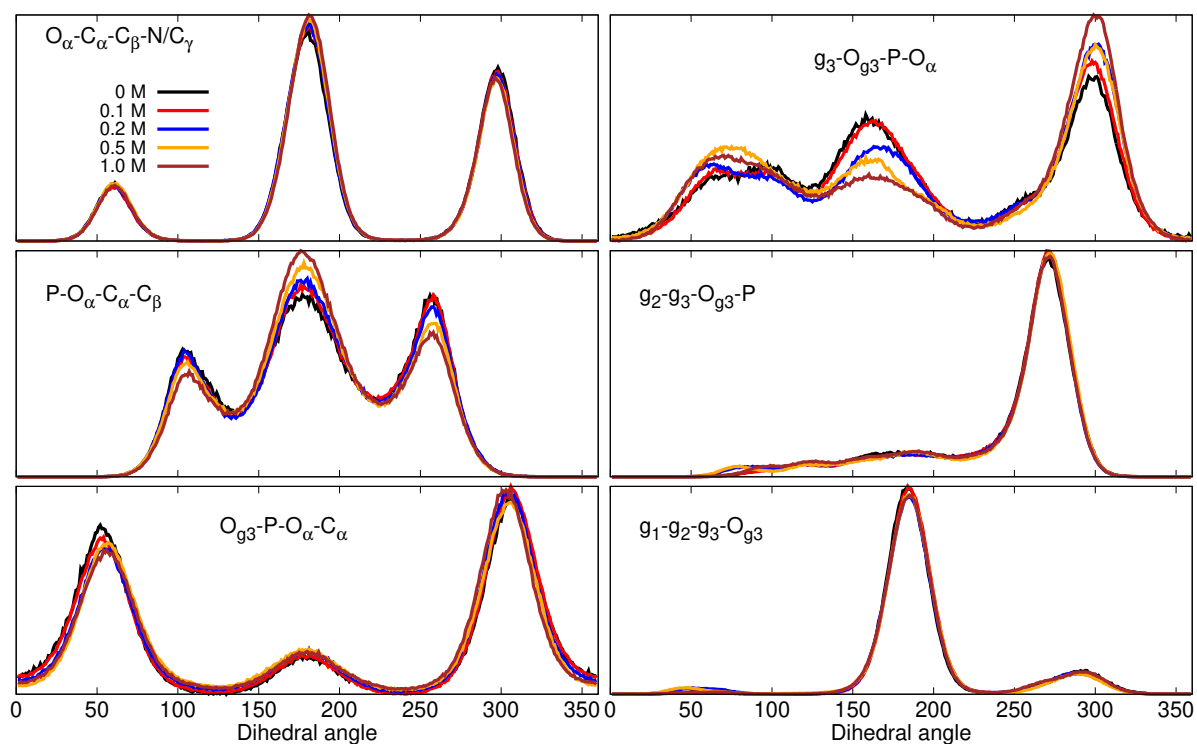


Figure S15: Changes in POPG Slipids dihedrals with increasing amount of CaCl_2 .

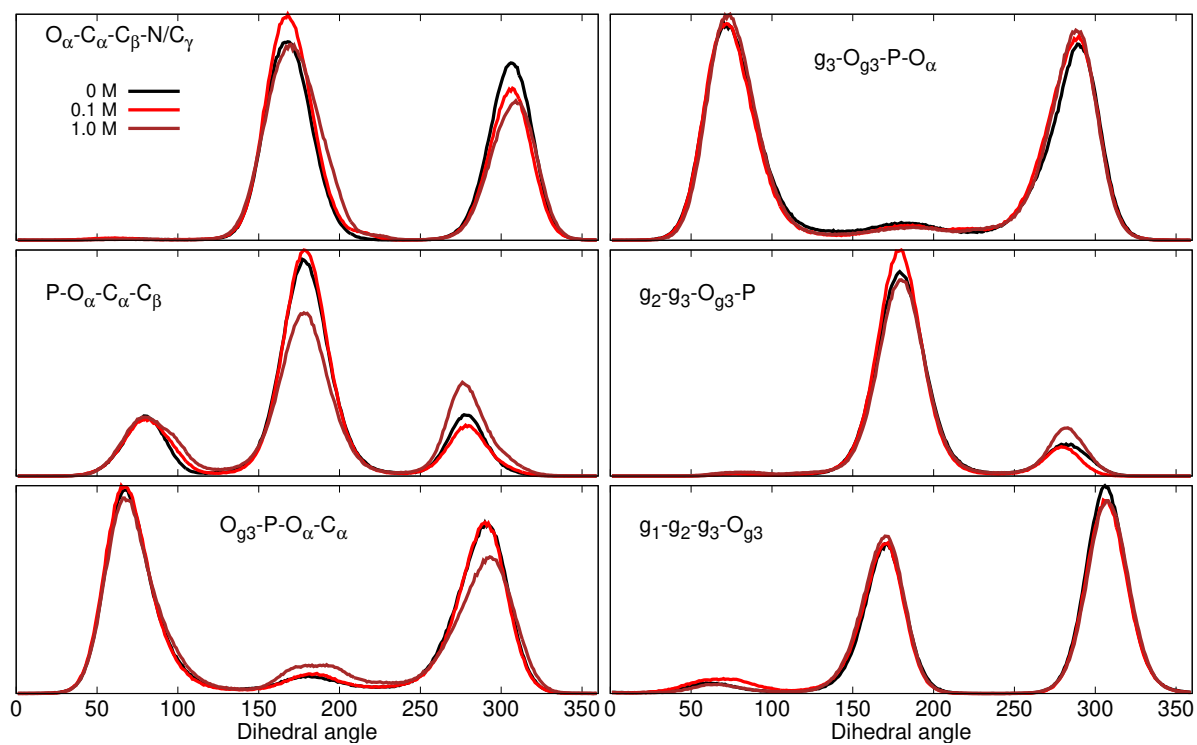


Figure S16: Changes in POPG lipid17 dihedrals with increasing amount of CaCl_2 .

S5 Simulated systems

The simulated systems of pure PE and PG bilayers without additional ions are listed in Tables S1 and S2, and lipid mixtures with additional ions in Table S3. The simulations were analyzed using preliminary versions of the NMRLipids databank (www.nmrlipids.fi, github.com/NMRLipids/MATCH and <https://github.com/NMRLipids/NMRLipidsIVPEandPG/tree/master/Data/Simulations>) and unique naming convention for lipid atoms (<http://nmrlipids.blogspot.com/2015/03/mapping-scheme-for-lipid-atom-names-for.html>), which enable automatic analysis of simulations with different force fields with varying atom naming conventions. The automatic analyses were implemented using MDAnalysis^{15,16} and MDTraj¹⁷ python libraries, and tools in the GROMACS software package.¹⁸ All codes are available from the project’s GitHub repository.¹⁹

The C–H bond order parameters were calculated directly from the carbon and hydrogen positions using the definition

$$S_{\text{CH}} = \frac{1}{2} \langle 3 \cos^2 \theta - 1 \rangle, \quad (1)$$

where θ is the angle between the C–H bond and the membrane normal (taken to align with z , with bilayer periodicity in the xy -plane). Angular brackets denote average over all sampled configurations. The order parameters were first calculated averaging over time separately for each lipid in the system. The average and the standard error of the mean were then calculated over different lipids. Code for all atom simulations is available in Ref. 20 (`scripts/calcOrderParameters.py`). For united atom simulations, we first constructed trajectories including hydrogens with ideal geometry using either `buildH` program²¹ or (`scratch/opAAUA_prod.py`) in Ref. 20, and the order parameters were then calculated from these trajectories. This approach has been tested against trajectories with explicit hydrogens and the deviations in order parameters are small.^{22,23}

Table S1: List of MD simulations with PE lipids.

| lipid | force field for lipids | ^a N _l | ^b N _w | ^c T (K) | ^d t _{sim} (ns) | ^e t _{anal} (ns) | ^f files |
|-------|--------------------------------|-----------------------------|-----------------------------|--------------------|------------------------------------|-------------------------------------|--------------------|
| POPE | CHARMM36 ²⁴ | 144 | 5760 | 310 | 500 | 400 | 25 |
| POPE | CHARMM36 ²⁴ | 500 | 25000 | 310 | 500 | 100 | 26 |
| POPE | CHARMM36-UA ²⁷ | 336 | 15254 | 310 | 2×200 | 2×100 | 28 |
| DPPE | Slipids ²⁹ | 288 | 9386 | 336 | 200 | 100 | 30 |
| POPE | Slipids ²⁹ | 336 | 15254 | 310 | 2×200 | 2×100 | 31 |
| POPE | Slipids ²⁹ | 500 | 25000 | 310 | 500 | 100 | 32 |
| DPPE | GROMOS-CKP ³³ | 128 | 3655 | 342 | 2×500 | 2×400 | 34 |
| POPE | GROMOS-CKP ³³ | 500 | 25000 | 310 | 500 | 100 | 35 |
| POPE | GROMOS 43A1-S3 ³⁶ | 128 | 3552 | 313 | 2×200 | 2×100 | 37 |
| POPE | OPLS-UA/HG-H ³⁸ | 128 | 3328 | 303 | 2×200 | 2×100 | 39 |
| POPE | OPLS-UA ³⁸ | 128 | 3328 | 303 | 2×200 | 2×100 | 40 |
| POPE | OPLS-MacRog ⁴¹ | 144 | 5760 | 310 | 500 | 350 | 42 |
| POPE | Berger-POPE-2004 ⁴³ | 128 | 3552 | 303 | 2×200 | 2×100 | 44 |
| POPE | Berger-POPE-2018 ⁴³ | 128 | 3552 | 303 | 2×200 | 2×100 | 45 |
| POPE | Lipid17 ⁴⁶ | 500 | 25000 | 310 | 500 | 100 | 47 |

^aNumber of lipid molecules^bNumber of water molecules^cSimulation temperature^dTotal simulation time^eTime used for analysis^fReference for simulation files**Table S2: List of MD simulations with PG lipids.**

| lipid/counter-ions | force field for lipids / ions | ^a N _l | ^b N _w | ^c T (K) | ^d t _{sim} (ns) | ^e t _{anal} (ns) | ^f files |
|----------------------|--|-----------------------------|-----------------------------|--------------------|------------------------------------|-------------------------------------|--------------------|
| POPG/K ⁺ | CHARMM36 ⁴⁸ | 118 | 4110 | 298 | 100 | 100 | 49 |
| POPG | CHARMM36 ⁴⁸ | 500 | 25000 | 310 | 500 | 100 | 50 |
| POPG/Na ⁺ | Slipids / Åqvist ^{51,52} | 288 | 10664 | 298 | 250 | 100 | 53 |
| DPPG/Na ⁺ | Slipids / Åqvist ^{51,52} | 288 | 11232 | 314 | 200 | 100 | 54 |
| DPPG/Na ⁺ | Slipids / Åqvist ^{51,52} | 288 | 11232 | 298 | 400 | 100 | 55 |
| POPG | Slipids / Åqvist ^{51,52} | 500 | 25000 | 310 | 500 | 100 | 56 |
| POPG | LIPID17 / Dang ^{46,57,58} | 500 | 25000 | 310 | 500 | 100 | 59 |
| POPG | GROMOS-CKP / GROMOS54A7 ^{33,60} | 500 | 25000 | 310 | 500 | 100 | 61 |

^aNumber of lipid molecules with largest mole fraction^bNumber of water molecules^cSimulation temperature^dTotal simulation time^eTime used for analysis^fReference for simulation files

Table S3: List of MD simulations with PE and PG lipids mixed with PC.

| lipid/counter-ions | force field for lipids / ions | CaCl ₂ (M) | ^a N _l | ^b N _w | ^c N _c | ^d T (K) | ^e t _{sim} (ns) | ^f t _{anal} (ns) | ^g files |
|--------------------|--|-----------------------|-----------------------------|-----------------------------|-----------------------------|--------------------|------------------------------------|-------------------------------------|--------------------|
| POPC | CHARMM36 ²⁴ | 0 | 500 | 25000 | 0 | 310 | 500 | 100 | ⁶² |
| POPC:POPG (7:3) | CHARMM36 ^{24,48} | 0 | 350 | 25000 | 0 | 310 | 500 | 100 | ⁶³ |
| POPC:POPG (1:1) | CHARMM36 ^{24,48} | 0 | 150:150 | 31500 | 0 | 298 | 500 | 400 | ⁶⁴ |
| POPC:POPG (1:1) | CHARMM36 ^{24,48} | 0.1 | 150:150 | 31329 | 57 | 298 | 400 | 300 | ⁶⁵ |
| POPC:POPG (1:1) | CHARMM36 ^{24,48} | 1.08 | 150:150 | 29766 | 578 | 298 | 500 | 400 | ⁶⁶ |
| POPC:POPG (4:1) | CHARMM36 ^{24,48} | 0 | 350:88 | 26280 | 0 | 298 | 500 | 400 | ⁶⁷ |
| POPC:POPG (4:1) | CHARMM36 ^{24,48} | 0.1 | 350:88 | 26280 | 47 | 298 | 500 | 400 | ⁶⁸ |
| POPC:POPG (4:1) | CHARMM36 ^{24,48} | 1.0 | 350:88 | 24927 | 451 | 298 | 500 | 400 | ⁶⁹ |
| POPC | CHARMM36 ²⁴ | 0 | 256 | 8704 | 0 | 300 | 300 | 250 | ⁷⁰ |
| POPC:POPE (1:1) | CHARMM36 ^{24,48} | 0 | 128 | 8704 | 0 | 300 | 300 | 250 | ⁷¹ |
| POPC | OPLS-MacRog ⁴¹ | 0 | 128 | 5120 | 0 | 300 | 500 | 300 | ⁷² |
| POPC:POPE (1:1) | OPLS-MacRog ⁴¹ | 0 | 128 | 5120 | 0 | 300 | 500 | 300 | ⁷³ |
| POPC | Slipid ²⁹ | 0 | 512 | 23943 | 0 | 298 | 170 | 100 | ⁷⁴ |
| POPC:POPE (1:1) | Slipid ²⁹ | 0 | 128 | 5120 | 0 | 298 | 500 | 300 | ⁷⁵ |
| POPC | GROMOS-CKP / ?? ^{76?} | 0 | 500 | 25000 | 0 | 310 | 500 | 100 | ⁷⁷ |
| POPC:POPG (7:3) | GROMOS-CKP / ?? ^{33,76?} | 0 | 350:150 | 25000 | 0 | 310 | 500 | 100 | ⁷⁸ |
| POPC | Slipid ²⁹ | 0 | 500 | 25000 | 0 | 310 | 500 | 100 | ⁷⁹ |
| POPC:POPG (7:3) | Slipid / Åqvist ^{29,52} | 0 | 350:150 | 25000 | 0 | 310 | 500 | 100 | ⁸⁰ |
| POPC:POPG (1:1) | Slipid / Dang ^{29,57,58,81} | 0 | 128:128 | 12800 | 0 | 298 | 500 | 400 | ⁸² |
| POPC:POPG (1:1) | Slipid / Dang ^{29,57,58,81} | 0.1 | 128:128 | 12800 | 23 | 298 | 500 | 400 | ⁸² |
| POPC:POPG (1:1) | Slipid / Dang ^{29,57,58,81} | 0.2 | 128:128 | 12800 | 46 | 298 | 1500 | 500 | ⁸² |
| POPC:POPG (1:1) | Slipid / Dang ^{29,57,58,81} | 0.5 | 128:128 | 12800 | 115 | 298 | 1500 | 500 | ⁸² |
| POPC:POPG (1:1) | Slipid / Dang ^{29,57,58,81} | 1.0 | 128:128 | 12800 | 230 | 298 | 1500 | 500 | ⁸² |
| POPC:POPG (4:1) | Lipid17 / Dang ^{46,57,58} | 0 | 350:88 | 26265 | 0 | 298 | 400 | 350 | ⁸³ |
| POPC:POPG (4:1) | Lipid17 / Dang ^{46,57,58} | 0.1 | 350:88 | 26124 | 47 | 298 | 400 | 250 | ⁸⁴ |
| POPC:POPG (4:1) | Lipid17 / Dang ^{46,57,58} | 1.0 | 350:88 | 24840 | 475 | 298 | 1200 | 200 | ⁸⁵ |
| POPC:POPG (1:1) | Lipid17 / Dang ^{46,57,58} | 0 | 150:150 | 31572 | 0 | 298 | 320 | 200 | ⁸⁶ |
| POPC:POPG (1:1) | Lipid17 / Dang ^{46,57,58} | 0.1 | 150:150 | 31401 | 57 | 298 | 718 | 198 | ⁸⁷ |
| POPC:POPG (1:1) | Lipid17 / Dang ^{46,57,58} | 1.0 | 150:150 | 29865 | 569 | 298 | 720 | 200 | ⁸⁸ |
| POPC:POPG (4:1) | Lipid17ecc / ECC-ions ⁸⁹⁻⁹¹ | 0 | 350:88 | 26265 | 0 | 298 | 400 | 300 | ⁹² |
| POPC:POPG (4:1) | Lipid17ecc / ECC-ions ⁸⁹⁻⁹¹ | 0.1 | 350:88 | 26124 | 47 | 298 | 400 | 300 | ⁹³ |
| POPC:POPG (4:1) | Lipid17ecc / ECC-ions ⁸⁹⁻⁹¹ | 1.0 | 350:88 | 24840 | 475 | 298 | 400 | 300 | ⁹⁴ |
| POPC:POPG (1:1) | Lipid17ecc / ECC-ions ⁸⁹⁻⁹¹ | 0 | 150:150 | 31572 | 0 | 298 | 347.8 | 333 | ⁹⁵ |
| POPC:POPG (1:1) | Lipid17ecc / ECC-ions ⁸⁹⁻⁹¹ | 0.1 | 150:150 | 29865 | 54 | 298 | 400 | 300 | ⁹⁶ |
| POPC:POPG (1:1) | Lipid17ecc / ECC-ions ⁸⁹⁻⁹¹ | 1.0 | 150:150 | 29865 | 569 | 298 | 600 | 400 | ⁹⁷ |
| POPC | Berger-POPC-07 ⁹⁸ | 0 | 256 | 10240 | 0 | 300 | 300 | 200 | ⁹⁹ |
| POPC:POPE (1:1) | Berger-POPE-04 ⁴³ | 0 | 128 | 11008 | 0 | 300 | 300 | 200 | ¹⁰⁰ |

^aNumber of lipid molecules with largest mole fraction

^bNumber of water molecules

^cNumber of additional cations

^dSimulation temperature

^eTotal simulation time

^fTime used for analysis

^gReference for simulation files

1.ion model for GROMOS-CKP?

S5.1 CHARMM36

POPE A lipid bilayer, consisting of a total of 144 POPE molecules, distributed equally between the two leaflets was set using CHARMM-GUI.¹⁰¹ The bilayer was solvated by 5760 water molecules (40 per lipid). The random initial configuration and topologies were generated using the CHARMM-GUI web portal, which provides GROMACS-compatible simulation input files.¹⁰¹ CHARMM36 lipid parameters²⁴ were used for POPE, whereas the CHARMM-specific TIP3P water model¹⁰² was used for water. The bilayer was simulated for 500 ns using GROMACS 2018.6 at 310 K.

The recommended simulation parameters for CHARMM36 force field in GROMACS were used.¹⁰¹ Namely, buffered Verlet lists were used to keep track of neighbouring atoms.¹⁰³ The Lennard-Jones potential was cut off at 1.2 nm with the forces switched to 0 between 1.0 nm and the cutoff value. The smooth PME algorithm^{104,105} was used to account for long-range electrostatics. The temperatures of the lipid and the solvent were separately coupled to a Nosé-Hoover thermostat^{106,107} with a time constant of 1 ps and a target temperature of 310 K. The system was coupled to a semi-isotropic (isotropic on the membrane plane) Parrinello–Rahman barostat¹⁰⁸ with a time constant of 5 ps, a reference pressure of 1 bar, and compressibility of 4.5×10^{-5} 1/bar. The bonds with hydrogen atoms were constrained using p-LINCS.^{109,110} The simulation files are available at Ref. 25.

POPG with 118 lipids Lipid bilayer containing 118 POPG molecules, 4110 TIP3P water molecules, and 118 potassium ions was build using CHARMM-GUI.¹⁰¹ The system was simulated 100 ns, coupled to 298 K using Nose-Hoover^{106,107} thermostat and 1 bar with semi-isotropic Parrinello-Rahman¹⁰⁸ pressure coupling. The used default parameters and force field files from CHARMM-GUI were used. The used files are available from 49.

POPG with 500 lipids A pure POPG system was built with CHARMM-GUI Membrane builder.¹⁰¹ A symmetric lipid distribution was used. The bilayer contains 500 lipids and 50 CHARMM TIP3P water molecules per lipid. The 500-ns-long production simulation was performed after energy minimization and equilibration. The last 100 ns was used for

analysis. For production simulation, a Leap-Frog algorithm was applied for integrating Newton’s equations of motion, and the LINCS algorithm was used to constrain all covalent bonds, allowing a time step of 2 fs. For water, the SETTLE method was applied. The simulation was performed in the NPT ensemble where the temperature was kept constant with the V-rescale thermostat.¹¹¹ Solvent and lipids were coupled to separate thermostats with a coupling constant of 0.1 ps. The pressure was kept constant with a semi-isotropic scheme. The Parrinello-Rahman barostat was used to keep the pressure at 1 bar with a coupling constant of 1 ps and a compressibility of $4.6 \times 10^5 \text{ bar}^{-1}$. Long-range electrostatic interactions with a real-space cutoff of 1.0 nm were treated by a particle mesh Ewald scheme (PME) with a Fourier spacing of 0.12 nm and a fourth-order interpolation to the Ewald mesh. Van der Waals interactions were treated with a Lennard-Jones (LJ) potential with a cutoff of 1.0 nm. Long-range dispersion correction to the pressure and energy was added.

POPC:POPE mixtures A pure POPC system and a 50:50 POPC:POPE mixture were built and equilibrated using CHARMM-GUI.¹⁰¹ They contained 256 lipids (for the mixture 64 lipids per leaflet for each species) and 34 water molecules per lipid. No ions were added. The production simulations were run for 300 ns with a time step of 2 fs. The first 50 ns were discarded for the analysis. The simulations were run with the GROMACS 2016.4¹¹² version. The v-rescale thermostat¹¹¹ was used with a temperature of 300 K and a time constant of 1 ps; lipids and water were coupled separately to the heat bath. Pressure was kept constant at 1 bar using a semi-isotropic Parrinello–Rahman barostat¹⁰⁸ with a time constant of 5.0 ps. A real space cut-off of 1.2 nm was employed for electrostatic interactions while the long-range part was evaluated using the PME method.^{104,105} A force-based switching function was used to switch the Lennard-Jones forces to zero over a range of 1–1.2 nm. All bonds with hydrogen atoms were constrained with the LINCS algorithm.^{109,110} Water molecules were kept rigid with the SETTLE algorithm.¹¹³ The simulation files are available from Ref. 70 (pure POPC) and 71 (POPC:POPE mixture).

POPC:POPG 1:1 and POPC:POPG 4:1 mixtures with additional calcium The initial structures

were built with CHARMM-GUI Membrane Builder.¹⁰¹ The TIP3P water model was used to solvate the systems. The simulations were run for 400 ns with timestep 2 fs and the first 100 ns were discarded as equilibration time. The simulations were run with GROMACS version 2020.2.¹¹⁴ The Nose-Hoover thermostat^{106,107} was used with temperature of 298 K and the time constant for temperature coupling was 1.0 ps. The semi-isotropic Parrinello-Rahman barostat¹⁰⁸ was used with reference pressure 1.0 bar and with a time constant of 5.0 ps with compressibility of $4.5\text{e-}5\text{ bar}^{-1}$. Long range electrostatic interactions were calculated with the PME method. All bonds with hydrogen atoms were constrained with LINCS algorithm. The simulation files are available from Refs. 64–69.

POPC and POPC:POPG (7:3) mixture Pure POPC bilayer and POPC:POPG (7:3) mixture were built with CHARMM-GUI Membrane builder.¹⁰¹ Both systems contained 500 lipids and 50 CHARMM TIP3P Water model per lipid. The 500-ns-long production simulation was performed after energy minimization and equilibration. The last 100 ns was used for analysis. For production simulation, a Leap-Frog algorithm was applied for integrating Newton’s equations of motion, and the LINCS algorithm was used to constrain all covalent bonds, allowing a time step of 2 fs. For water, the SETTLE method was applied. All simulations were performed in the NPT ensemble where the temperature was kept constant with the V-rescale thermostat.¹¹¹ Solvent and lipids were coupled to separate thermostats with a coupling constant of 0.1 ps. The pressure was kept constant with a semi-isotropic scheme. The Parrinello-Rahman barostat was used to keep the pressure at 1 bar with a coupling constant of 1 ps and a compressibility of $4.6 \times 10^{-5}\text{ bar}^{-1}$. Long-range electrostatic interactions with a real-space cutoff of 1.0 nm were treated by a particle mesh Ewald scheme (PME) with a Fourier spacing of 0.12 nm and a fourth-order interpolation to the Ewald mesh. van der Waals interactions were treated with a Lennard-Jones (LJ) potential with a cutoff of 1.0 nm. Long-range dispersion correction to the pressure and energy was added.

POPC and cationic surfactant (dihexadecyldimethylammonium) mixture Initial structures were taken from similar previously published¹² simulations with Amber lipid14 force field,

which are available from Ref. 115–120. Default simulations parameters and force field files from CHARMM-GUI¹⁰¹ were used, except for dihexadecyldimethylammonium for which the atom types and partial charges of Amber lipid14 parameters from previous work¹² were modified to correspond Charmm36 force field. Systems contained 50 POPC molecules, 3983 water molecules, and 12, 30, 44, or 88 dihexadecyldimethylammonium molecules. Chloride ions were used as counterions for dihexadecyldimethylammonium. Reference system without cationic surfactants contained 200 POPC and 9000 water molecules. Systems were simulated 200 ns (the first 20 ns was discarded as an equilibration period) using Gromacs 5¹¹² at the temperature of 313 K. All simulation files are available from Refs. 121,122.

S5.2 CHARMM36-UA

POPE CHARMM36-UA POPE simulations were performed for 200 ns using GROMACS version 5.0.6. A topology for POPE was constructed using the standard CHARMM36 all-atom PE head group combined with the original CHARMM36-UA lipid tail parameters.²⁷ Simulations were performed using a hexagonal periodic box containing 336 POPE lipids. This membrane was constructed using a MARTINI force field¹²³ coarse-grained self-assembly simulation followed by reverse-mapping to an atomic resolution. Simulations were performed using standard CHARMM lipid simulation settings; further details and simulation data are available at Ref. 28.

S5.3 Slipids

POPE Slipids POPE simulations were performed for 200 ns using GROMACS version 5.0.6. Simulations employed the original Slipids POPE parameters²⁹ and the same starting structure as the CHARMM36-UA POPE simulations. Slipids simulations employed standard AMBER force field cut-offs of 1.0 nm, previously validated for use with the Slipids force field.²³ Further simulation details and data are available at Ref. 31.

DPPE with 288 lipids. The starting structure for simulation with 288 DPPE lipids and 9386

water molecules was constructed with the MEMBRANE BUILDER website.¹²⁴ The TIP3P¹⁰² water model was used to solvate the system. Simulation was performed for 200 ns, and the last 100 ns were used for the analysis. Simulation was carried out within the NPT ensemble using the GROMACS 5.0.4 package.¹¹² Timestep of 2 fs was used with the leapfrog integrator. The Nosé–Hoover thermostat^{106,107} was used with reference temperature of 336 K and a relaxation time constant of 0.5 ps; lipids and water were coupled separately to the heat bath. Pressure was kept constant at 1.013 bar using a semi-isotropic Parrinello–Rahman barostat¹⁰⁸ with a time constant of 10.0 ps. Long-range electrostatic interactions were calculated using the PME method.^{104,105} A real space cut-off of 1.0 nm was employed with grid spacing of 0.12 nm in the reciprocal space. Lennard-Jones potentials were cut off at 1.4 nm, with a dispersion correction applied to both energy and pressure. All covalent bonds in lipids were constrained using the LINCS algorithm,¹¹⁰ whereas water molecules were constrained using SETTLE.¹¹³ Twin-range cutoffs, 1.0 nm and 1.6 nm, were used for the neighbor lists with the long-range neighbor list updated every 10 steps.

POPG with 288 lipids. The starting structure for simulation with 288 POPG lipids, 10664 water molecules and 288 Na ions was constructed with the MEMBRANE BUILDER website.¹²⁴ The TIP3P¹⁰² water model was used to solvate the system and Ions are described by the parameters derived by Åqvist.⁵² Simulation was performed for 250 ns, and the last 100 ns were used for the analysis. Same simulation conditions as DPPE with reference temperature of 298 K.

DPPG with 288 lipids. The starting structure for simulation with 288 DPPG lipids, 11232 water molecules and 288 Na ions was constructed with the MEMBRANE BUILDER website.¹²⁴ The TIP3P¹⁰² water model was used to solvate the system and Ions are described by the parameters derived by Åqvist.⁵² For the 298 K temperature, simulation was performed for 400 ns, and the last 100 ns were used for the analysis. For the 314 K temperature, simulation was performed for 200 ns, and the last 100 ns were used for the analysis. Same simulation conditions as DPPE for both temperatures.

POPC:POPE mixture A POPC/POPE bilayer with its lipids distributed evenly among the leaflets was generated by from a pure POPC bilayer by removing and renaming atoms in the head group region. The bilayer contained a total of 100 POPC and 100 POPE lipids, and it was solvated by 45 water molecules per lipid (for a total of 9000 water molecules). The Slipids force field^{29,51,125} was used for lipids, and the TIP3P model¹⁰² for water. A 300 ns-long simulation was performed using GROMACS 2019.4.¹¹² The simulation parameters were equal to those used for the POPC/POPG mixture with additional CaCl_2 (see below). The simulation data are available at Ref. 75.

POPC:POPG mixture with additional CaCl_2 A lipid bilayer consisting of a total of 256 lipids (128 POPC + 128 POPG) spread equally between the two leaflets was generated using CHARMM-GUI.¹⁰¹ The membrane was solvated by 50 water molecules per lipid (a total of 12800), and 128 Na^+ counter ions for the POPG charges. The initial random configuration was equilibrated using the CHARMM-GUI protocol and using the CHARMM36 force field.²⁴ Next, additional ions were added to obtain initial CaCl_2 concentrations of 0, 100, 200, 500, or 1000 mM (0/0, 23/46, 46/92, 115/230, 230/460 $\text{Ca}^{2+}/\text{Cl}^-$ ions) The systems were energy-minimized and equilibrated using the Slipids force field^{29,51,125} before production simulations at 298 K. The ion parameters by Dang et al. were used.⁵⁸

The neighbour lists with a cutoff of 1.0 nm were updated every 10 simulation steps. The smooth PME algorithm was used to calculate long-range electrostatics.^{104,105} The Lennard-Jones potential was cut off at 1.0 nm, and the dispersion corrections¹²⁶ were applied to energy and pressure. The stochastic velocity rescaling thermostat¹¹¹ with a time constant of 0.5 ps and a target temperature of 298 K was applied separately to lipids and the solvent. A constant pressure of 1 bar was maintained by a Parrinello–Rahman barostat¹⁰⁸ with a time constant of 10 ps and compressibility of 4.5×10^{-5} 1/bar. The pressure coupling was performed semi-isotropically with the two simulation box vectors aligned along the membrane plane considered isotropic. All bonds were constrained using the p-LINCS algorithm.^{109,110}

The systems simulated for 1500 ns (CaCl_2 -containing systems) or 500 ns (systems without

CaCl₂). The simulations were performed using GROMACS 2019.4,¹¹² and the simulation files are available at Ref. 82.

S5.4 Berger

Following the earlier convention in the NMRlipids Project,¹ for the Berger-based models we use the following naming convention: Berger - {*molecule name*} - {*year when model published first time*} {*citation*}.

POPE Simulations of POPE membranes using the Berger force field employed two variants of the Berger force field for PE lipids. The first (Berger-POPE-2004) used the de Vries modifications which includes additional repulsive Lennard-Jones interactions on the ethanolamine hydrogen atoms.⁴³ The second (Berger-POPE-2018) used this same approach but doubled the repulsive strength employed for the hydrogen atom van der Waals interactions.⁴⁵ The latter variant results in more disorder within the membrane and a closer agreement with experimental properties such as the area per lipid of POPE. POPE simulations were performed for 200 ns using GROMACS 5.0.6 and employed a POPE membrane with 64 lipids per leaflet taken from a published GROMOS-CKP POPE membrane.³³ Simulations used a 1.0 nm cut-off for both electrostatic and van der Waals interactions with PME and a dispersion correction for the energy and pressure employed respectively. Further simulation details can be found at Ref. 44 for Berger-POPE-2004 and at Ref. 45 for Berger-POPE-2018.

POPC:POPE mixtures Two systems were simulated using the Berger force field,¹²⁷ pure POPC and a mixture 50:50 POPC:POPE. For POPC, parameters with the Bachar¹²⁸ correction for the dihedrals next to double bond were used (Berger-POPC-07). For POPE, we additionally used the de Vries modification implementing a repulsion of the hydrogen atoms located on the amino group of ethanolamine.⁴³ Starting from a PDB file of a pure POPC system with Berger atom names, a 50:50 POPC:POPE mixture was built by mutating randomly methyl groups to hydrogens (POPC → POPE). Each system contained 256 lipids (for the mixture 64 lipids per leaflet for each species) and about 40 water molecules per lipid. No ions were

added. Both systems were minimized and equilibrated. The production simulations were run for 300 ns with a time step of 2 fs. The first 100 ns were discarded for the analysis. The simulations were run with GROMACS 4.5.3¹²⁹ version. The v-rescale thermostat¹¹¹ was used with a temperature of 300 K and a time constant of 0.1 ps; lipids and water were coupled separately to the heat bath. Pressure was kept constant at 1 bar using a semi-isotropic Parrinello-Rahman barostat¹⁰⁸ with a time constant of 4.0 ps. A real space cut-off of 1.0 nm was employed for van der Waals and electrostatic interactions. The long-range part of electrostatic interactions was evaluated using the PME method^{104,105} with a grid spacing of 0.12 nm and an interpolation order of 4. All bonds with hydrogen atoms were constrained with the LINCS algorithm.^{109,110} Water molecules were kept rigid with the SETTLE algorithm.¹¹³ The simulation files are available from Ref. 99 (pure POPC) and 100 (POPC:POPE mixture).

S5.5 GROMOS 43A1-S3

POPE GROMOS 43A1-S3 simulations were performed for 200 ns using GROMACS 4.0.7 employing the standard GROMOS 43A1-S3 POPE force field.³⁶ The simulation structure had 64 lipids per leaflet and was constructed from a GROMOS 43A1-S3 POPC membrane.⁷⁶ Simulations employed standard GROMOS 43A1-S3 settings. Further details and simulation data can be found at Ref. 37.

S5.6 OPLS-UA

POPE POPE simulations with the OPLS-UA force field were performed for 200 ns using GROMACS 4.5.7. POPE parameters were constructed by modifying the OPLS-UA POPC of Ulmschneider and Ulmschneider³⁸ with standard OPLS lysine parameters. The starting membrane structure, containing 64 POPE lipids per leaflet, was created by modifying an OPLS-UA POPC membrane. Simulations employed a 1.0 nm cut-off with PME and no dispersion correction. Further simulation details and data can be found at 40.

POPE with vdW interaction in H (OPLS-UA/HG-H) In addition to the OPLS simulations

mentioned above, further simulations employing the same starting structure and simulation settings were employed using slightly modified parameters. These modified parameters, termed OPLS-UA/HG-H, were designed to increase the area per lipid through employing a small repulsive potential on the ethanolamine hydrogen atoms, as per the approach of de Vries with the Berger POPE parameters.⁴³ Further details and data of these simulations can be found at Ref. 39.

S5.7 GROMOS-CKP

POPE Pure POPE system was built with CHARMM-GUI Membrane builder.¹⁰¹ Symmetric lipid distribution was used. The bilayer contains 500 lipids and 50 SPC Water model per lipid. GROMOS-CKP force field was used for lipids.³³ The 500-ns-long production simulation was performed after energy minimization and equilibration. The last 100 ns was used for analysis. For production simulation, a Leap-Frog algorithm was applied for integrating Newton’s equations of motion, and the LINCS algorithm was used to constrain all covalent bonds, allowing a time step of 2 fs. For water, the SETTLE method was applied. The simulation was performed in the NPT ensemble where the temperature was kept constant with the V-rescale thermostat.¹¹¹ Solvent and lipids were coupled to separate thermostats with a coupling constant of 0.1 ps. The pressure was kept constant with a semi-isotropic scheme. The Parrinello-Rahman barostat was used to keep the pressure at 1 bar with a coupling constant of 1 ps and a compressibility of $4.6 \times 10^5 \text{ bar}^{-1}$. Long-range electrostatic interactions with a real-space cutoff of 1.0 nm were treated by a particle mesh Ewald scheme (PME) with a Fourier spacing of 0.12 nm and a fourth-order interpolation to the Ewald mesh. van der Waals interactions were treated with a Lennard-Jones (LJ) potential with a cutoff of 1.0 nm. Long-range dispersion correction to the pressure and energy was added. The simulation data and files are available at Ref. 35.

DPPE GROMOS-CKP DPPE simulations were performed for 500 ns using GROMACS 5.0.6. These simulations used the original GROMOS-CKP parameters³³ but with the charges

in the ethanolamine head group taken from a GROMOS 53A6 lysine side-chain rather than a PC lipid head group, as done in the original parameters. The starting structure contained 64 lipids per leaflet and was taken from a previous GROMOS-CKP simulation.³³ Simulations employed standard GROMOS-CKP settings with PME employed for the long-range electrostatic interactions. Further details and simulation data can be found at Ref. 34.

POPG A pure L-POPG system was built with CHARMM-GUI Membrane builder.¹⁰¹ A symmetric lipid distribution was used. The bilayer contains 500 lipids and 50 SPC Water model per lipid with 500 sodium ions. GROMOS-CKP force field was used for lipid³³ and GROMOS54A7⁶⁰ for the rest. The 500-ns-long production simulation was performed after energy minimization and equilibration. The last 100 ns was used for analysis. The simulation details are the same as in POPE system. The data and simulation files are available at Ref. 61.

POPC:POPG mixture **2.Simulation details by A. Peon.**

S5.8 OPLS-MacRog

POPE A bilayer patch with a total of 144 POPE molecules, distributed evenly between two leaflets, was created by reordering atoms in a final structure of a POPE simulation performed using the CHARMM36 force field. The bilayer was hydrated by 40 water molecules per lipid for a total of 5760 water molecules. The OPLS-based MacRog force field was used¹³⁰ for lipids and the TIP3P model¹⁰² for water.

Buffered Verlet lists¹⁰³ were used to keep track of neighbours. The Lennard-Jones potential was cut off at 1.0 nm, and dispersion corrections were applied to energy and pressure.¹²⁶ Smooth PME algorithm was used to calculate long-range electrostatics.^{104,105} The Nosé–Hoover thermostat was used to keep the temperatures of the lipids and water at 310 K. These groups were coupled separately, and a time constant of 0.4 ps was used. The Parrinello–Rahman barostat¹⁰⁸ was used to keep the pressures in the membrane plane as well as normal

to it constant at 1 bar. For the barostat, a time constant of 10 ps was used, and the membrane compressibility was set to 4.5×10^{-5} 1/bar. All bonds were constrained using p-LINCS.^{109,110}

The system was simulated for 500 ns using GROMACS 2019.2,¹¹² and the simulation data are available at Ref. 42.

POPC:POPE mixtures The initial force field parameter files in GROMACS format were taken from Ref. 41. However, a number of errors were detected in the published files so we fixed them in the following way. For POPE, the two aliphatic chains sn-1 and sn-2 were switched (in the file the lipid was in fact OPPE); one atom (named C27) was not connected to the previous atom in the aliphatic chain so bonds, angles, dihedrals, pairs were included to create the connection; two atoms were called C27 thus one of them was renamed C28. For POPC, some impropers were missing leading to non planar systems for double bonds (in particular the carbonyls of sn-1 and sn-2 as well as the double bond of the oleoyl chain), we thus added back those impropers. The resulting fixed files can be found from Refs. 72 (popc_fixed.itp) and 73 (pope_fixed.itp). To check our fix, one simulation of pure POPC was also run and the order parameter compared to previous published results.¹ We found very similar values. All the details of the procedure described here are described in file *scratch/report_results_comparison.pdf* in Ref. 19.

Two systems of pure POPC and 50:50 POPC:POPE mixture were built using CHARMM-GUI.¹⁰¹ They contained 128 lipids and 5120 TIP3 water molecules. The initial PDB file was modified to match OPLS-MacRog nomenclature and atom order. No ions were added. The production simulations were run for 500 ns with a time step of 2 fs. The first 200 ns were discarded for the analysis. The simulations were run with the GROMACS 2018.5¹¹² version. The v-rescale thermostat¹¹¹ was used with a temperature of 300 K and a time constant of 0.1 ps; lipids and water were coupled separately to the heat bath. Pressure was kept constant at 1 bar using a semi-isotropic Parrinello-Rahman barostat¹⁰⁸ with a time constant of 4.0 ps. Long-range electrostatic interactions were calculated using the PME method.^{104,105} A real space cut-off of 1.0 nm was employed with a grid spacing of 0.1 nm in the reciprocal

space. Lennard-Jones potentials were cut off at 1.0 nm. All covalent bonds in lipids were constrained using the LINCS algorithm.^{109,110} Water molecules were kept rigid with the SETTLE algorithm.¹¹³

The data for pure POPC are available from Refs. 72, and for the POPC:POPE mixture from Ref. 73.

S5.9 Lipid17

POPE A pure POPE system built with CHARMM-GUI was used to create the Amber input files. Amber prmtop and inpcrd files were obtained with LEaP from AmberTools 16 distribution (<http://ambermd.org/>). ParmEd version 3.0.0¹³¹ was used to convert the Amber prmtop and inpcrd files into Gromacs top and gro files. After conversion, the incorrect dihedrals with type 1 were changed to type 9 (for details, see discussion in <https://github.com/NMRLipids/NMRLipidsIVPEandPG/issues/12>).

The bilayer contains 500 lipids and 50 TIP3P waters per lipid. The 500-ns-long production simulation was performed after energy minimization and equilibration. The last 100 ns was used for analysis. For production simulation, a Leap-Frog algorithm was applied for integrating Newton’s equations of motion, and the LINCS algorithm was used to constrain all covalent bonds, allowing a time step of 2 fs. For water, the SETTLE method was applied. The simulation was performed in the NPT ensemble where the temperature was kept constant with the V-rescale thermostat.¹¹¹ Solvent and lipids were coupled to separate thermostats with a coupling constant of 0.1 ps. The pressure was kept constant with a semi-isotropic scheme. The Parrinello-Rahman barostat was used to keep the pressure at 1 bar with a coupling constant of 1 ps and a compressibility of $4.6 \times 10^5 \text{ bar}^{-1}$. Long-range electrostatic interactions with a real-space cutoff of 1.0 nm were treated by a particle mesh Ewald scheme (PME) with a Fourier spacing of 0.12 nm and a fourth-order interpolation to the Ewald mesh. van der Waals interactions were treated with a Lennard-Jones (LJ) potential with a cutoff of 1.0 nm. Long-range dispersion correction to the pressure and energy was added.

POPG A pure POPG system built with CHARMM-GUI was used to create the Amber input files. The system was further processed and simulated similarly to the POPE system.

POPC:POPG 4:1 and POPC:POPG 1:1 mixtures with different CaCl_2 concentrations Initial structures were built by removing appropriate amount of lipids from POPC:POPG 7:3 mixture available from Ref. 132, which was built similarly to pure POPG and POPE systems. Force field parameters from the same reference (Amber prmtop and inpcrd files were obtained with LEaP from AmberTools 16 distribution (<http://ambermd.org/>) and converted to Gromacs top and gro files with ParmEd version 3.0.0¹³¹) were used, except that incorrect dihedrals with type 1 were changed to type 9 (for details, see discussion in <https://github.com/NMRLipids/NMRLipidsIVPEandPG/issues/12>). Simulations were performed using the Gromacs simulation package¹¹⁴ with the time step of 2 fs. The non-bonded interactions were calculated directly within 1.0 nm cutoff; the Verlet scheme was used;¹⁰³ and the long-range electrostatic forces were calculated using particle mesh Ewald.¹⁰⁵ The bond lengths of hydrogen atoms were constrained using LINCS.¹¹⁰ Temperature was coupled to the velocity rescaling thermostat¹¹¹ at 298 K with a coupling constant of 1 ps. Pressure was coupled to the Parrinello–Rahman barostat¹⁰⁸ at 1 bar with a coupling constant of 10 ps. For simulations with CaCl_2 , appropriate amount of ions with Dang^{57,58} parameters were added into the solvent. The simulation files are available from Refs. 83–88

S5.10 Lipid17ecc

POPC:POPG 4:1 and POPC:POPG 1:1 mixtures with different CaCl_2 concentrations Implicit inclusion of electronic polarizability by electronic continuum correction (ECC), implemented by scaling the partial charges in force fields, can be used to improve ion interactions with lipids and other biomolecules in classical MD simulations.¹³³ For Amber Lipid14/17 force fields, ECC has been previously implemented by scaling the charges and Lennard-Jones σ s of headgroup, glycerol backbone, and carbonyl regions by constant factors.^{12,13} Here, we apply similar ECC approach to Amber Lipid17 PG parameters as done previously for PS:¹³ charges

and Lennard-Jones σ s of headgroup, glycerol backbone, and carbonyl regions of parameters POPG from Ref. 132 were scaled by factors of $f_q=0.75$ and $f_\sigma=0.89$, respectively (and the dihedral types were corrected to type 9 as in previous section). Previously introduced ECC-POPC parameters (scaling factors $f_q=0.8$ and $f_\sigma=0.89$ applied to Lipid14 POPC parameters) were used for POPC.¹² ECC-ion parameters with the scaled charges^{89–91} from bitbucket.org/hseara/ions/src/master/, and SPC/E water model¹³⁴ were used in these simulations. Rest of the simulation parameters and initial configurations were taken from Lipid17 simulations.^{83–88} Simulation files of Lipid17ecc simulations are available from Refs. 92–97.

S6 Author contributions

Amélie Bacle set up, performed and analysed POPC and POPC:POPE (1:1) simulations with the Berger Force Field.

Pavel Buslaev performed the analysis of dihedrals and isomers of lipids. Analysed lipid structures from Protein Data Bank. Prepared panels for figures 2 and 4. Participated in discussions.

Rebeca García Fandiño designed and supervised the molecular dynamics simulations carried out by Antonio Peón, and contributed to some discussions.

Fernando Favela-Rosales set up and performed DPPE, POPG and DPPG simulations with the Slipids Force Field.

Tiago M. Ferreira was responsible for the solid-state NMR experiments/figures and took part in writing the manuscript.

Patrick F.J. Fuchs supervised Paula Milán Rodríguez, Amélie Bacle and Chris Papadopoulos, created the buildH software, contributed to many discussions.

Ivan Gushchin supervised Pavel Buslaev and contributed to the analysis of lipid structures in the Protein Data Bank.

Matti Javanainen set up and performed simulations using CHARMM36, Slipids, and MacRog lipid models. He contributed to the organization of the manuscript.

Anne M. Kiirikki set up and performed POPC:POPG(1:1) and POPC:POPG(4:1) simulations with CHARMM36 and POPC:POPG(4:1) with Lipid17ecc. She also contributed to the NMRlipids databank.

Jesper J. Madsen set up, performed, and analysed several of the CHARMM36 simulations. Provided comments on the manuscript.

Josef Melcr

Paula Milán Rodríguez set up, performed and analysed POPC and POPC:POPE (1:1) simulations with the MacRog Force Field. She also fixed the initial force field (itp) files prior to the simulations.

Markus S. Miettinen

O. H. Samuli Ollila designed the project and managed the work. Ran and analysed several simulations. Wrote the manuscript.

Chris G. Papadopoulos set up, performed and analysed POPC and POPC:POPE (1:1) simulations with the CHARMM36 Force Field.

Antonio Peón set up, performed and analysed POPC, POPE, POPG and POPC:POPG (7:3) simulations with the CHARMM36, SLIPIDS, GROMOS-CKP and Lipid17 Force Fields.

Thomas J. Piggot Setup and performed many of the PE simulations including those with Berger, CHARMM36-UA, GROMOS 43A1-S3, GROMOS-CKP, and OPLS-UA force fields.

Ángel Piñeiro Created the opAAUA_prod.py code for the calculation of order parameters. Contributed to some discussions.

Salla I. Virtanen

References

- (1) Botan, A.; Favela-Rosales, F.; Fuchs, P. F. J.; Javanainen, M.; Kanduč, M.; Kulig, W.; Lamberg, A.; Loison, C.; Lyubartsev, A.; Miettinen, M. S. et al. Toward Atomistic Resolution Structure of Phosphatidylcholine Headgroup and Glycerol Backbone at Different Ambient Conditions. *J. Phys. Chem. B* **2015**, *119*, 15075–15088.
- (2) Antila, H.; Buslaev, P.; Favela-Rosales, F.; Ferreira, T. M.; Gushchin, I.; Javanainen, M.; Kav, B.; Madsen, J. J.; Melcr, J.; Miettinen, M. S. et al. Headgroup Structure and Cation Binding in Phosphatidylserine Lipid Bilayers. *J. Phys. Chem. B* **2019**, *123*, 9066–9079.
- (3) Wohlgemuth, R.; Waespe-Sarcevic, N.; Seelig, J. Bilayers of phosphatidylglycerol. A deuterium and phosphorus nuclear magnetic resonance study of the head-group region. *Biochemistry* **1980**, *19*, 3315–3321.

- (4) Seelig, J.; Gally, H. U. Investigation of phosphatidylethanolamine bilayers by deuterium and phosphorus-31 nuclear magnetic resonance. *Biochemistry* **1976**, *15*, 5199–5204.
- (5) Gally, H. U.; Pluschke, G.; Overath, P.; Seelig, J. Structure of Escherichia coli membranes. Glycerol auxotrophs as a tool for the analysis of the phospholipid head-group region by deuterium magnetic resonance. *Biochemistry* **1981**, *20*, 1826–1831.
- (6) Ollila, O. S.; Pabst, G. Atomistic resolution structure and dynamics of lipid bilayers in simulations and experiments. *Biochim. Biophys. Acta* **2016**, *1858*, 2512 – 2528.
- (7) Borle, F.; Seelig, J. Ca²⁺ binding to phosphatidylglycerol bilayers as studied by differential scanning calorimetry and ²H- and ³¹P-nuclear magnetic resonance. *Chem. Phys. Lipids* **1985**, *36*, 263 – 283.
- (8) Scherer, P.; Seelig, J. Structure and dynamics of the phosphatidylcholine and the phosphatidylethanolamine head group in L-M fibroblasts as studied by deuterium nuclear magnetic resonance. *EMBO J.* **1987**, *6*.
- (9) Macdonald, P. M.; Seelig, J. Calcium binding to mixed phosphatidylglycerol-phosphatidylcholine bilayers as studied by deuterium nuclear magnetic resonance. *Biochemistry* **1987**, *26*, 1231–1240.
- (10) Seelig, J.; MacDonald, P. M.; Scherer, P. G. Phospholipid head groups as sensors of electric charge in membranes. *Biochemistry* **1987**, *26*, 7535–7541.
- (11) Catte, A.; Girysh, M.; Javanainen, M.; Loison, C.; Melcr, J.; Miettinen, M. S.; Monticelli, L.; Maatta, J.; Oganessian, V. S.; Ollila, O. H. S. et al. Molecular electrometer and binding of cations to phospholipid bilayers. *Phys. Chem. Chem. Phys.* **2016**, *18*, 32560–32569.
- (12) Melcr, J.; Martinez-Seara, H.; Nencini, R.; Kolafa, J.; Jungwirth, P.; Ollila, O. H. S.

- Accurate Binding of Sodium and Calcium to a POPC Bilayer by Effective Inclusion of Electronic Polarization. *J. Phys.Chem. B* **2018**, *122*, 4546–4557.
- (13) Melcr, J.; Ferreira, T. M.; Jungwirth, P.; Ollila, O. H. S. Improved Cation Binding to Lipid Bilayers with Negatively Charged POPS by Effective Inclusion of Electronic Polarization. *J. Chem. Theo. Comput.* **2020**, *16*, 738–748.
- (14) Akutsu, H.; Seelig, J. Interaction of metal ions with phosphatidylcholine bilayer membranes. *Biochemistry* **1981**, *20*, 7366–7373.
- (15) Michaud-Agrawal, N.; Denning, E. J.; Woolf, T. B.; Beckstein, O. MDAanalysis: A toolkit for the analysis of molecular dynamics simulations. *J. Comput. Chem.* **2011**, *32*, 2319–2327.
- (16) Richard J. Gowers,; Max Linke,; Jonathan Barnoud,; Tyler J. E. Reddy,; Manuel N. Melo,; Sean L. Seyler,; Jan DomaÅŹski,; David L. Dotson,; SÅľbastien Buchoux,; Ian M. Kenney, et al. MDAanalysis: A Python Package for the Rapid Analysis of Molecular Dynamics Simulations. Proceedings of the 15th Python in Science Conference. 2016; pp 98 – 105.
- (17) McGibbon, R. T.; Beauchamp, K. A.; Harrigan, M. P.; Klein, C.; Swails, J. M.; Hernandez, C. X.; Schwantes, C. R.; Wang, L.-P.; Lane, T. J.; Pande, V. S. MDTraj: A Modern Open Library for the Analysis of Molecular Dynamics Trajectories. *Biophys. J.* **2015**, *109*, 1528 – 1532.
- (18) Abraham, M.; van der Spoel, D.; Lindahl, E.; Hess, B.; the GROMACS development team, GROMACS user manual version 5.0.7. 2015.
- (19) project, N. NMRLipidsIVb GitHub repository. <https://github.com/NMRLipids/NMRLipidsIVPEandPG>.

- (20) Ollila, O. H. S.; et al., MATCH GitHub repository. <https://github.com/NMRLipids/MATCH>.
- (21) Santuz, H.; Bacle, A.; Poulain, P.; Fuchs, P. buildH (v1.2.0): Build hydrogens from a united- atom MD of lipids and calculate the order parameter. 2021; <https://doi.org/10.5281/zenodo.4676218>.
- (22) Fuchs, P. Validation of buildH on a CHARMM36 POPC trajectory. 2021; <https://doi.org/10.5281/zenodo.4715962>.
- (23) Piggot, T. J.; Allison, J. R.; Sessions, R. B.; Essex, J. W. On the Calculation of Acyl Chain Order Parameters from Lipid Simulations. *J. Chem. Theory Comput.* **2017**, *13*, 5683–5696.
- (24) Klauda, J. B.; Venable, R. M.; Freites, J. A.; O'Connor, J. W.; Tobias, D. J.; Mondragon-Ramirez, C.; Vorobyov, I.; MacKerell Jr, A. D.; Pastor, R. W. Update of the CHARMM All-Atom Additive Force Field for Lipids: Validation on Six Lipid Types. *J. Phys. Chem. B* **2010**, *114*, 7830–7843.
- (25) Javanainen, M. Simulation of a POPE bilayer at 310K with the CHARMM36 force field. 2019; <https://doi.org/10.5281/zenodo.2641987>.
- (26) Peón, A. CHARMM36 POPE Bilayer Simulation (Last 100 ns, 310 K). 2019; <https://doi.org/10.5281/zenodo.3237461>.
- (27) Lee, S.; Tran, A.; Allsopp, M.; Lim, J. B.; Henin, J.; Klauda, J. B. CHARMM36 United Atom Chain Model for Lipids and Surfactants. *J. Phys. Chem. B* **2014**, *118*, 547–556.
- (28) Piggot, T. CHARMM36-UA POPE Simulations (versions 1 and 2) 310 K (NOTE: hexagonal membrane and POPE is called PEUA). 2018; <https://doi.org/10.5281/zenodo.1293774>.

- (29) Jämbeck, J. P. M.; Lyubartsev, A. P. An Extension and Further Validation of an All-Atomistic Force Field for Biological Membranes. *J. Chem. Theory Comput.* **2012**, *8*, 2938–2948.
- (30) Favela-Rosales, F. MD simulation trajectory of a fully hydrated DPPE bilayer: SLIPIDS, Gromacs 5.0.4. 2017. 2017; <https://doi.org/10.5281/zenodo.495247>.
- (31) Piggot, T. Slipids POPE Simulations (versions 1 and 2) 310 K (NOTE: hexagonal membrane). 2018; <https://doi.org/10.5281/zenodo.1293813>.
- (32) Peón, A. SLIPID POPE Bilayer Simulation (Last 100 ns, 310 K). 2019; <https://doi.org/10.5281/zenodo.3231342>.
- (33) Piggot, T. J.; Holdbrook, D. A.; Khalid, S. Electroporation of the *E. coli* and *S. aureus* membranes: Molecular Dynamics Simulations of Complex Bacterial Membranes. *J. Phys. Chem. B* **2011**, *115*, 13381–13388.
- (34) Piggot, T. GROMOS-CKP DPPE Simulations (versions 1 and 2) 342 K. 2018; <https://doi.org/10.5281/zenodo.1293957>.
- (35) Peón, A. GROMOS POPE Bilayer Simulation (Last 100 ns, 310 K). 2019; <https://doi.org/10.5281/zenodo.3237754>.
- (36) Chiu, S.-W.; Pandit, S. A.; Scott, H. L.; Jakobsson, E. An Improved United Atom Force Field for Simulation of Mixed Lipid Bilayers. *J. Phys. Chem. B* **2009**, *113*, 2748–2763.
- (37) Piggot, T. GROMOS 43A1-S3 POPE Simulations (versions 1 and 2) 313 K (NOTE: anisotropic pressure coupling). 2018; <https://doi.org/10.5281/zenodo.1293762>.
- (38) Ulmschneider, J. P.; Ulmschneider, M. B. United Atom Lipid Parameters for Combination with the Optimized Potentials for Liquid Simulations All-Atom Force Field. *J. Chem. Theory Comput.* **2009**, *5*, 1803–1813.

- (39) Piggot, T. OPLS-UA POPE Simulations (versions 1 and 2) 303 K with vdW on H atoms. 2018; <https://doi.org/10.5281/zenodo.1293853>.
- (40) Piggot, T. OPLS-UA POPE Simulations (versions 1 and 2) 303 K. 2018; <https://doi.org/10.5281/zenodo.1293855>.
- (41) RÅsg, T.; OrÅĆowski, A.; Llorente, A.; Skotland, T.; SylvÅdnne, T.; Kauhanen, D.; Ekroos, K.; Sandvig, K.; Vattulainen, I. Data including GROMACS input files for atomistic molecular dynamics simulations of mixed, asymmetric bilayers including molecular topologies, equilibrated structures, and force field for lipids compatible with OPLS-AA parameters. *Data in Brief* **2016**, *7*, 1171 – 1174.
- (42) Javanainen, M. Simulation of a POPE bilayer, lipid model based on OPLS-aa by Rog et al. 2019; <https://doi.org/10.5281/zenodo.3571071>.
- (43) de Vries, A. H.; Mark, A. E.; Marrink, S. J. The Binary Mixing Behavior of Phospholipids in a Bilayer: A Molecular Dynamics Study. *The Journal of Physical Chemistry B* **2004**, *108*, 2454–2463.
- (44) Piggot, T. Berger POPE Simulations (versions 1 and 2) 303 K - de Vries repulsive H. 2018; <https://doi.org/10.5281/zenodo.1293889>.
- (45) Piggot, T. Berger POPE Simulations (versions 1 and 2) 303 K - larger repulsive H. 2018; <https://doi.org/10.5281/zenodo.1293891>.
- (46) Gould, I.; Skjevik, A.; Dickson, C.; Madej, B.; Walker, R. Lipid17: A Comprehensive AMBER Force Field for the Simulation of Zwitterionic and Anionic Lipids. 2018; In preparation.
- (47) Peón, A. LIPID17 POPE Bilayer Simulation (Last 100 ns, 310 K) using dihedral 9. 2019; <https://doi.org/10.5281/zenodo.4424292>.

- (48) Venable, R. M.; Luo, Y.; Gawrisch, K.; Roux, B.; Pastor, R. W. Simulations of Anionic Lipid Membranes: Development of Interaction-Specific Ion Parameters and Validation Using NMR Data. *J. Phys. Chem. B* **2013**, *117*, 10183–10192.
- (49) Ollila, O. H. S. POPG lipid bilayer simulation at T298K ran with MODEL_CHARMM_GUI force field and Gromacs. 2017; <https://doi.org/10.5281/zenodo.1011096>.
- (50) Peón, A. CHARMM36 POPG Bilayer Simulation (Last 100 ns, 310 K). 2019; <https://doi.org/10.5281/zenodo.3237463>.
- (51) Jämbeck, J. P. M.; Lyubartsev, A. P. Implicit inclusion of atomic polarization in modeling of partitioning between water and lipid bilayers. *Phys. Chem. Chem. Phys.* **2013**, *15*, 4677–4686.
- (52) Åqvist, J. Ion-water interaction potentials derived from free energy perturbation simulations. *J. Phys. Chem.* **1990**, *94*, 8021–8024.
- (53) Favela-Rosales, F. MD simulation trajectory of a fully hydrated POPG bilayer: SLIPIDS, Gromacs 5.0.4. 2017. 2017; <https://doi.org/10.5281/zenodo.546133>.
- (54) Favela-Rosales, F. MD simulation trajectory of a fully hydrated DPPG bilayer @314K: SLIPIDS, Gromacs 5.0.4. 2017. 2017; <https://doi.org/10.5281/zenodo.546136>.
- (55) Favela-Rosales, F. MD simulation trajectory of a fully hydrated DPPG bilayer @298K: SLIPIDS, Gromacs 5.0.4. 2017. 2017; <https://doi.org/10.5281/zenodo.546135>.
- (56) PeÅşn, A. LIPID17 POPG Bilayer Simulation (Last 100 ns, 310 K) using dihedral type 9. 2019; <https://doi.org/10.5281/zenodo.3832274>.
- (57) Smith, D. E.; Dang, L. X. Computer simulations of NaCl association in polarizable water. *J. Chem. Phys* **1994**, *100*, 3757–3766.

- (58) Dang, L. X.; Schenter, G. K.; Glezakou, V.-A.; Fulton, J. L. Molecular simulation analysis and X-ray absorption measurement of Ca²⁺, K⁺ and Cl⁻ ions in solution. *J. Phys. Chem. B* **2006**, *110*, 23644–54.
- (59) PeÅšn, A. LIPID17 POPG Bilayer Simulation (Last 100ns, 310 K) using dihedral type 9 instead of type 1. 2020; <https://doi.org/10.5281/zenodo.3832219>.
- (60) Schmid, N.; Eichenberger, A. P.; Choutko, A.; Riniker, S.; Winger, M.; Mark, A. E.; van Gunsteren, W. F. Definition and testing of the GROMOS force-field versions 54A7 and 54B7. *European Biophysics Journal* **2011**, *40*, 843.
- (61) Peón, A. GROMOS POPG Bilayer Simulation (Last 100 ns, 310 K). 2019; <https://doi.org/10.5281/zenodo.3266166>.
- (62) Peón, A. CHARMM36 POPC Bilayer Simulation (Last 100 ns, 310 K). 2019; <https://doi.org/10.5281/zenodo.3247813>.
- (63) Peón, A. CHARMM36 POPC-POPG 7:3 Bilayer Simulation (Last 100 ns, 310 K). 2019; <https://doi.org/10.5281/zenodo.3248689>.
- (64) Kiirikki, A. M.; Ollila, O. H. S. POPC:POPG 1:1 MD simulation with CHARMM36 in water and Na⁺ counter ions. 2020; <https://doi.org/10.5281/zenodo.3997116>.
- (65) Kiirikki, A. M.; Ollila, O. H. S. POPC:POPG 1:1 MD simulation with CHARMM36 in 0.1 M CaCL solution and Na⁺ counter ions. 2020; <https://doi.org/10.5281/zenodo.4005515>.
- (66) Kiirikki, A. M.; Ollila, O. H. S. POPC:POPG 1:1 MD simulation with CHARMM36 in 1 M CaCL solution and Na⁺ counter ions. 2020; <https://doi.org/10.5281/zenodo.3997135>.
- (67) Kiirikki, A. M.; Ollila, O. H. S. POPC:POPG 4:1 MD simulation with CHARMM36 in water with Na⁺ counter ions. 2020; <https://doi.org/10.5281/zenodo.3996952>.

- (68) Kiirikki, A. M.; Ollila, O. H. S. POPC:POPG 4:1 MD simulation with CHARMM36 in 0.1 M CaCl₂ solution with Na⁺ counter ions. 2020; <https://doi.org/10.5281/zenodo.3997019>.
- (69) Kiirikki, A. M.; Ollila, O. H. S. POPC:POPG 4:1 MD simulation with CHARMM36 in 1 M CaCl₂ solution with Na⁺ counterions. 2020; <https://doi.org/10.5281/zenodo.3997037>.
- (70) Papadopoulos, C.; Fuchs, P. F. CHARMM36 pure POPC MD simulation (300 K - 300ns - 1 bar). 2018; <https://doi.org/10.5281/zenodo.1306800>.
- (71) Papadopoulos, C.; Fuchs, P. F. CHARMM36 POPC/POPE (50%-50%) MD simulation (300 K - 300ns - 1 bar). 2018; <https://doi.org/10.5281/zenodo.1306821>.
- (72) Milán Rodríguez, P.; Fuchs, P. F. J. MacRog pure POPC MD simulation (300 K - 500ns - 1 bar). 2020; <https://doi.org/10.5281/zenodo.3741793>.
- (73) Milán Rodríguez, P.; Fuchs, P. F. J. MacRog POPC/POPE 1:1 MD simulation (300 K - 500ns - 1 bar). 2020; <https://doi.org/10.5281/zenodo.3725637>.
- (74) Favela-Rosales, F. MD simulation trajectory of a lipid bilayer: Pure POPC in water. SLIPIDS, Gromacs 4.6.3. 2016. 2016; <https://doi.org/10.5281/zenodo.166034>.
- (75) Javanainen, M. Simulation of POPC:POPE 1:1 membrane with the Slipids force field. 2020; <https://doi.org/10.5281/zenodo.3605386>.
- (76) Piggot, T. J.; Piñeiro, Á.; Khalid, S. Molecular Dynamics Simulations of Phosphatidylcholine Membranes: A Comparative Force Field Study. *J. Chem. Theory Comput.* **2012**, *8*, 4593–4609.
- (77) Peón, A. GROMOS-CKP POPC Bilayer Simulation (Last 100 ns, 310 K). 2019; <https://doi.org/10.5281/zenodo.3247435>.

- (78) Peón, A. GROMOS-CKP POPC-POPG 7:3 Bilayer Simulation (Last 100 ns, 310 K). 2019; <https://doi.org/10.5281/zenodo.3266240>.
- (79) Peón, A. SLIPID POPC Bilayer Simulation (Last 100 ns, 310 K). 2019; <https://doi.org/10.5281/zenodo.3235552>.
- (80) Peón, A. SLIPID POPC-POPG 7:3 Bilayer Simulation (Last 100 ns, 310 K). 2019; <https://doi.org/10.5281/zenodo.3240156>.
- (81) Jämbeck, J. P.; Lyubartsev, A. P. Another piece of the membrane puzzle: extending slipids further. *J. Chem. Theo. Comput.* **2012**, *9*, 774–784.
- (82) Javanainen, M. Simulations of POPC:POPG 1:1 membranes with varying levels of CaCl₂ using the Slipids force field. 2020; <https://doi.org/10.5281/zenodo.3613573>.
- (83) Virtanen, S.; Ollila, O. H. S. LIPID17 POPC-POPG 80:20 MD simulation, Na⁺ counterions, 298K. 2019; <https://doi.org/10.5281/zenodo.3693681>.
- (84) Virtanen, S.; Ollila, O. H. S. LIPID17 POPC-POPG 80:20 MD simulation, Na⁺ counterions and 100mM CaCl₂, 298K. 2019; <https://doi.org/10.5281/zenodo.3833725>.
- (85) Virtanen, S.; Ollila, O. H. S. LIPID17 POPC-POPG 80:20 MD simulation, Na⁺ counterions and 1000mM CaCl₂, 298K. 2019; <https://doi.org/10.5281/zenodo.3874378>.
- (86) Virtanen, S.; Ollila, O. H. S. LIPID17 POPC-POPG 50:50 MD simulation, Na⁺ counterions, 298K. 2019; <https://doi.org/10.5281/zenodo.3857816>.
- (87) Virtanen, S.; Ollila, O. H. S. LIPID17 POPC-POPG 50:50 MD simulation, Na⁺ counterions and 100mM CaCl₂, 298K. 2019; <https://doi.org/10.5281/zenodo.3871590>.

- (88) Virtanen, S.; Ollila, O. H. S. LIPID17 POPC-POPG 50:50 MD simulation, Na⁺ counterions and 1000mM CaCl₂, 298K. 2019; <https://doi.org/10.5281/zenodo.3864993>.
- (89) Pluhařová, E.; Fischer, H. E.; Mason, P. E.; Jungwirth, P. Hydration of the chloride ion in concentrated aqueous solutions using neutron scattering and molecular dynamics. *Mol. Phys.* **2014**, *112*, 1230–1240.
- (90) Kohagen, M.; Mason, P. E.; Jungwirth, P. Accounting for Electronic Polarization Effects in Aqueous Sodium Chloride via Molecular Dynamics Aided by Neutron Scattering. *J. Phys. Chem. B* **2016**, *120*, 1454–1460.
- (91) Martínek, T.; Duboué-Dijon, E.; Timr, Š.; Mason, P. E.; Baxová, K.; Fischer, H. E.; Schmidt, B.; Pluhařová, E.; Jungwirth, P. Calcium ions in aqueous solutions: Accurate force field description aided by ab initio molecular dynamics and neutron scattering. *J. Chem. Phys.* **2018**, *148*, 222813.
- (92) Kiirikki, A. M.; Ollila, O. H. S. Lipid17ecc POPC:POPG 4:1 MD simulation in water with Na⁺ counter ions. 2020; <https://doi.org/10.5281/zenodo.3997154>.
- (93) Kiirikki, A. M.; Ollila, O. H. S. Lipid17ecc POPC:POPG 4:1 bilayer simulation in 0.1 M CaCl₂ solution and Na⁺ counter ions. 2020; <https://doi.org/10.5281/zenodo.3997176>.
- (94) Kiirikki, A. M.; Ollila, O. H. S. Lipid17ecc POPC:POPG 4:1 bilayer simulation in 1 M CaCl₂ solution and Na⁺ counter ions. 2020; <https://doi.org/10.5281/zenodo.4492639>.
- (95) Ollila, O. H. S.; Virtanen, I. S. ECC-LIPID17 POPC-POPG 50:50 MD simulation, Na⁺ counterions, 298K. 2020; <https://doi.org/10.5281/zenodo.3859339>.

- (96) Ollila, O. H. S.; Virtanen, I. S. ECC-LIPID17 POPC-POPG 50:50 MD simulation, Na⁺ counterions and 100mM CaCl₂, 298K. 2020; <https://doi.org/10.5281/zenodo.3855729>.
- (97) Ollila, O. H. S.; Virtanen, I. S. ECC-LIPID17 POPC-POPG 50:50 MD simulation, Na⁺ counterions and 1000mM CaCl₂, 298K. 2020; <https://doi.org/10.5281/zenodo.3862036>.
- (98) Ollila, S.; Hyvönen, M. T.; Vattulainen, I. Polyunsaturation in Lipid Membranes: Dynamic Properties and Lateral Pressure Profiles. *J. Phys. Chem. B* **2007**, *111*, 3139–3150.
- (99) Bacle, A.; Fuchs, P. F. J. Berger pure POPC MD simulation (300 K - 300ns - 1 bar). 2018; <https://doi.org/10.5281/zenodo.1402417>.
- (100) Bacle, A.; Fuchs, P. F. J. Berger POPC/POPE (50:50 ratio) MD simulation (300 K - 400ns - 1 bar). 2018; <https://doi.org/10.5281/zenodo.1402449>.
- (101) Lee, J.; Cheng, X.; Swails, J. M.; Yeom, M. S.; Eastman, P. K.; Lemkul, J. A.; Wei, S.; Buckner, J.; Jeong, J. C.; Qi, Y. et al. CHARMM-GUI Input Generator for NAMD, GROMACS, AMBER, OpenMM, and CHARMM/OpenMM Simulations Using the CHARMM36 Additive Force Field. *J. Chem. Theo. Comput.* **2016**, *12*, 405–413.
- (102) Jorgensen, W. L.; Chandrasekhar, J.; Madura, J. D.; Impey, R. W.; Klein, M. L. Comparison of simple potential functions for simulating liquid water. *J. Chem. Phys.* **1983**, *79*, 926–935.
- (103) Páll, S.; Hess, B. A flexible algorithm for calculating pair interactions on {SIMD} architectures. *Comput. Phys. Commun.* **2013**, *184*, 2641 – 2650.
- (104) Darden, T.; York, D.; Pedersen, L. Particle mesh Ewald: An N·log(N) method for Ewald sums in large systems. *J. Chem. Phys.* **1993**, *98*, 10089–10092.

- (105) Essman, U. L.; Perera, M. L.; Berkowitz, M. L.; Larden, T.; Lee, H.; Pedersen, L. G. A smooth particle mesh ewald potential. *J. Chem. Phys.* **1995**, *103*, 8577–8592.
- (106) Nose, S. A molecular dynamics method for simulations in the canonical ensemble. *Mol. Phys.* **1984**, *52*, 255–268.
- (107) Hoover, W. G. Canonical dynamics: Equilibrium phase-space distributions. *Phys. Rev. A* **1985**, *31*, 1695–1697.
- (108) Parrinello, M.; Rahman, A. Polymorphic transitions in single crystals: A new molecular dynamics method. *J. Appl. Phys.* **1981**, *52*, 7182–7190.
- (109) Hess, B. P-LINCS: A Parallel Linear Constraint Solver for Molecular Simulation. *J. Chem. Theory Comput.* **2008**, *4*, 116–122.
- (110) Hess, B.; Bekker, H.; Berendsen, H. J. C.; Fraaije, J. G. E. M. LINCS: a linear constraint solver for molecular dynamics simulations. *J. Comput. Chem.* **1997**, *18*, 1463–1472.
- (111) Bussi, G.; Donadio, D.; Parrinello, M. Canonical sampling through velocity rescaling. *J. Chem. Phys.* **2007**, *126*.
- (112) Abraham, M. J.; Murtola, T.; Schulz, R.; Páll, S.; Smith, J. C.; Hess, B.; Lindahl, E. GROMACS: High performance molecular simulations through multi-level parallelism from laptops to supercomputers. *SoftwareX* **2015**, *1*, 19–25.
- (113) Miyamoto, S.; Kollman, P. A. SETTLE: An analytical Version of the SHAKE and RATTLE Algorithm for Rigid Water Models. *J. Comput. Chem* **1992**, *13*, 952–962.
- (114) Páll, S.; Zhmurov, A.; Bauer, P.; Abraham, M.; Lundborg, M.; Gray, A.; Hess, B.; Lindahl, E. Heterogeneous parallelization and acceleration of molecular dynamics simulations in GROMACS. *J. Chem. Phys.* **2020**, *153*, 134110.
- (115) Ollila, O. H. S. POPC bilayer simulated at T313K with the Lipid14 model using Gromacs. 2017; <https://doi.org/10.5281/zenodo.1020709>.

- (116) Ollila, O. H. S. POPC bilayer with 10% of dihexadecyldimethylammonium simulated at T313K with the Lipid14 model using Gromacs. 2017; <https://doi.org/10.5281/zenodo.1020240>.
- (117) Ollila, O. H. S. POPC bilayer with 20% of dihexadecyldimethylammonium simulated at T313K with the Lipid14 model using Gromacs. 2017; <https://doi.org/10.5281/zenodo.1020593>.
- (118) Ollila, O. H. S. POPC bilayer with 30% of dihexadecyldimethylammonium simulated at T313K with the Lipid14 model using Gromacs. 2017; <https://doi.org/10.5281/zenodo.1020623>.
- (119) Ollila, O. H. S. POPC bilayer with 42% of dihexadecyldimethylammonium simulated at T313K with the Lipid14 model using Gromacs. 2017; <https://doi.org/10.5281/zenodo.1020671>.
- (120) Ollila, O. H. S. POPC bilayer with 50% of dihexadecyldimethylammonium simulated at T313K with the Lipid14 model using Gromacs. 2017; <https://doi.org/10.5281/zenodo.1020689>.
- (121) Ollila, POPC CHARMM36 T313K. 2020; <https://doi.org/10.5281/zenodo.4040423>.
- (122) Ollila, O. H. S. CHARMM36 simulations of POPC mixed with cationic surfactant. 2018; <https://doi.org/10.5281/zenodo.1288297>.
- (123) Marrink, S.; Risselada, H.; Yefimov, S.; Tieleman, D.; de Vries, A. The MARTINI forcefield: coarse grained model for biomolecular simulations. *J. Phys. Chem. B* **2007**, *111*, 7812–7824.
- (124) Ghahremanpour, M. M.; Arab, S. S.; Aghazadeh, S. B.; Zhang, J.; van der Spoel, D. MemBuilder: a web-based graphical interface to build heterogeneously mixed membrane

- bilayers for the GROMACS biomolecular simulation program. *Bioinformatics* **2013**, *30*, 439–441.
- (125) Jämbeck, J. P. M.; Lyubartsev, A. P. Derivation and Systematic Validation of a Refined All-Atom Force Field for Phosphatidylcholine Lipids. *J. Phys. Chem. B* **2012**, *116*, 3164–3179.
- (126) Shirts, M. R.; Mobley, D. L.; Chodera, J. D.; Pande, V. S. Accurate and Efficient Corrections for Missing Dispersion Interactions in Molecular Simulations. *J. Phys. Chem. B* **2007**, *111*, 13052–13063.
- (127) Berger, O.; Edholm, O.; Jähnig, F. Molecular dynamics simulations of a fluid bilayer of dipalmitoylphosphatidylcholine at full hydration, constant pressure, and constant temperature. *Biophys. J.* **1997**, *72*, 2002 – 2013.
- (128) Bachar, M.; Brunelle, P.; Tieleman, D. P.; Rauk, A. Molecular Dynamics Simulation of a Polyunsaturated Lipid Bilayer Susceptible to Lipid Peroxidation. *J. Phys. Chem. B* **2004**, *108*, 7170–7179.
- (129) Pronk, S.; Páll, S.; Schulz, R.; Larsson, P.; Bjelkmar, P.; Apostolov, R.; Shirts, M. R.; Smith, J. C.; Kasson, P. M.; van der Spoel, D. et al. GROMACS 4.5: a high-throughput and highly parallel open source molecular simulation toolkit. *Bioinformatics* **2013**, *29*, 845–854.
- (130) Kulig, W.; Pasenkiewicz-Gierula, M.; Róg, T. Cis and trans unsaturated phosphatidylcholine bilayers: A molecular dynamics simulation study. *Chem. Phys. Lipids* **2016**, *195*, 12 – 20.
- (131) Shirts, M. R.; Klein, C.; Swails, J. M.; Yin, J.; Gilson, M. K.; Mobley, D. L.; Case, D. A.; Zhong, E. D. Lessons learned from comparing molecular dynamics engines on the SAMPL5 dataset. *Journal of Computer-Aided Molecular Design* **2017**, *31*, 147–161.

- (132) Peón, A. LIPID17 POPC-POPG 7:3 Bilayer Simulation (Last 100 ns, 150 mM NaCl, 310 K). 2019; <https://doi.org/10.5281/zenodo.2585523>.
- (133) Dubou  l-Dijon, E.; Javanainen, M.; Delcroix, P.; Jungwirth, P.; Martinez-Seara, H. A practical guide to biologically relevant molecular simulations with charge scaling for electronic polarization. *J. Chem. Phys.* **2020**, *153*, 050901.
- (134) Berendsen, H. J. C.; Grigera, J. R.; Straatsma, T. P. The missing term in effective pair potentials. *J. Phys. Chem.* **1987**, *91*, 6269–6271.